2018

In-Situ Treatment of 1,4-Dioxane Under Column Scale Conditions

Michaela A. Cashman
University of Rhode Island, michaela.cashman@gmail.com

IN-SITU TREATMENT OF 1,4-DIOXANE UNDER COLUMN SCALE CONDITIONS

BY

MICHAELA A. CASHMAN

A THESIS SUBMITTED IN PARTIAL FULFILLMENT OF THE

REQUIREMENTS FOR THE DEGREE OF

MASTER OF SCIENCE

IN

BIOLOGICAL AND ENVIRONMENTAL SCIENCE

UNIVERSITY OF RHODE ISLAND

2018

MASTER OF BIOLOGICAL AND ENVIRONMENTAL SCIENCE

OF

MICHAELA A. CASHMAN

APPROVED:

Thesis Committee:

Major Professor: Thomas Boving

Soni Pradhanang

Vinka Craver

Nasser H. Zawia

DEAN OF THE GRADUATE SCHOOL

UNIVERSITY OF RHODE ISLAND

2018

ABSTRACT

There is limited understanding of the underlying process that govern the peroxone activated persulfate (PAP) oxidation of 1,4-Dioxane, specifically at what rates this advanced oxidation process (AOP) proceeds, how long the system remains active once injected into a contaminant plume, and which radicals might be involved. The research presented herein investigates a peroxone activated persulfate oxidant, patented by EnChem Engineering (Newton, Massachusetts) under the name OxyZone®, and its effect on 1,4-Dioxane contaminated water under column scale conditions in the presence of porous material. A secondary objective of this study was to identify radicals formed during the oxidation of 1,4-Dioxane using OxyZone with Electron Paramagnetic Resonance (EPR) spectroscopy. Initial batch experiments provided data on the reaction rates as a function of the oxidant: contaminant ratio. The formation of hydroxyl radicals, and possibly sulfate radicals, was confirmed by EPR. Subsequent flow-through column-scale experiments were conducted in a sand packed, 1.5 m long PVC column saturated with an aqueous solution containing dissolved approximately 300 µ/L 1,4-Dioxane. 1,4-Dioxane effluent concentrations were monitored with a Gas Chromatograph-Mass Spectrometer. Two types of column scale experiments were performed to simulate two possible oxidant injection schemes, namely oxidant injection at one or more than one locations within the flow field of a 1,4-Dioxane plume. In these column experiments, the oxidation rates varied from 0.08 $h^{-1}$to 1.54 h^{-1} and were greatest when the oxidant was injected as two slugs farthest up-gradient. Under these conditions, almost all 1,4-Dioxane was destroyed during breakthrough of the oxidant solution. Most noteworthy is that the

degradation process continued past the time expected from the breakthrough of a conservative tracer. The prolonged reactivity was found to be caused by the oxidant solution's elevated density (about 1.05 g/cm^3), which retarded the (upward) flow of the oxidant solution through the column, thereby extending the contact time with the contaminant and decreasing the 1,4-Dioxane concentration to below detection limit during much of the oxidant breakthrough. Together, this research suggests that the in-situ chemical oxidation of 1,4-Dioxane in groundwater plumes with peroxone activated persulfate is possible. However, field application must account for the density driven transport that influences the oxidant transport.

ACKNOWLEDGMENTS

Above all, I would like to thank my advisor, Dr. Thomas Boving for his continued support throughout my time as a student. I am deeply appreciative of your mentorship and guidance throughout these past three years, and I look forward to future collaborations. I would also like to thank my committee, Dr. Soni Pradhanang, Dr. Vinka Craver, and Dr. Miriam Reumann for their support.

I extend my sincerest gratitude and thanks to Dr. Louis Kirschenbaum and Justin Holowachuk of the Department of Chemistry for their willingness to share their expertise and resources. I would also like to thank the US EPA's Pollution Elimination Branch for their analytic guidance. Specifically, I would like to thank Dr. Mark Cantwell and David Katz for their help in the laboratory. I must also thank Dr. Raymond Ball of EnChem Engineering Inc. for his technical guidance and support.

Many thanks must be given to my mentors and colleagues within the Department of Geosciences. Thank-you Dr. Dylan Eberle for your help in establishing my project. Thank-you Dr. Anne Veeger for your technical guidance. And a special thank-you goes to Dr. David Fastovsky, for handing me a ukulele on days that I needed it.

Finally, I would like to thank my "home-team". Thank-you to my family, my partner Andrew, and Rachel. I would like to dedicate this manuscript to my grandmother, Anna M. Kane. Thank-you for always trusting in my abilities.

PREFACE

This thesis is written in manuscript format in accordance with the requirements of the Graduate School of the University of Rhode Island. This thesis contains one manuscript and a series of appendices. The thesis, entitled *In-situ treatment of 1,4-Dioxane under column scale conditions*, is prepared for submission to the journal *Chemosphere*.

TABLE OF CONTENTS

List of Figures

List of Tables

MANUSCRIPT- I

IN-SITU TREATMENT OF 1,4-DIOXANE UNDER COLUMN SCALE CONDITIONS

Prepared for submission to *Chemosphere*

INTRODUCTION

1.1 BACKGROUND

1,4-Dioxane is a heterocyclic organic contaminant found in groundwater plumes at industrial sites worldwide. This cyclic ether (Figure 1) was historically used in many industrial products and processes, including usage as a stabilizer or a wetting and dispersing agent for textile processing and printing (Anderson et al., 2012; Klečka and Gonsior, 1986; Mohr et al., 2016). In 1985, approximately 90% of 1,4-Dioxane produced was used as a stabilizer for chlorinated solvents, particularly 1,1,1-trichloroethane (1,1,1-TCA) and to some extent trichloroethylene (TCE) (Figure 2) (EPA, 1995; Mohr et al., 2016). Both 1,1,1-TCA and TCE are synthetic, chlorinated aliphatic compounds used primarily as industrial degreaser in the past. In case of 1,1,1-TCA, as much as 3.5% (by volume) 1,4-Dioxane has been added to this solvent (HSDB, 1995; Mohr, 2001). Chlorinated solvents, such as 1,1,1-TCA and TCE, are found at approximately 80% of all EPA Superfund sites with groundwater contamination (SERDP, 2006). Historic records of poor handling, storage, and disposal practices of chlorinated solvents highlights the significant potential for 1,4-Dioxane contamination in groundwater.

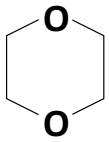

Figure 1: 1,4-Dioxane, a heterocyclic either with a molecular mass of 88.11 grams per mole.

Figure 2: 2a. Trichloroethylene, a double-bonded chlorinated hydrocarbon with a molecular mass of 131. 5 grams per mole, and 2b. 1,1,1-Trichloroethane a single-bonded chlorinated hydrocarbon with a molecular mass of 133.4 grams per mole.

Under the Clean Air Act amendment of 1990, production of 1,1,1-TCA was halted, with the exception of use for essential applications in the United States. Since 1990, annual production of 1,1,1-TCA decreased from 300 million pounds to 125 million pounds in 2005 (HSIA, 2004). TCE is still used at significantly lower volumes for industrial purposes. In a review conducted by the United States Airforce (USAF), 1,4-Dioxane was observed in 17.4% of groundwater monitoring wells with records for TCE or TCA, which accounts for 93.7% of all 1,4-Dioxane detections (Anderson et al., 2012). 1,4-Dioxane frequently occurs with 1,1,-dichloroethane (DCA), a byproduct of 1,1,1-TCA degradation (Adamson et al., 2017; Anderson et al., 2012; EPA, 2013).

While 1,4-Dioxane is a regulated hazardous material and 2B Probable Carcinogen, it is not currently classified as a US EPA priority pollutant, and does not have a maximum contaminant level (MCL) for drinking water (EPA, 2013; IARC, 1999; Mohr et al., 2016). Many states have developed screening levels for 1,4-Dioxane, but state regulated thresholds vary over an order of magnitude (Suthersan et al., 2016). While there are no federal standards for 1,4-Dioxane in groundwater, the EPA has established drinking water advisories. The EPA 1-day health advisory is 4 mg/L of 1,4-Dioxane in drinking water, whereas the 10-day health advisory is 0.4 mg/L. The lifetime health advisory for 1,4-Dioxane in drinking water is 0.2 mg/L. Because of its widespread occurrence, 1,4-Dioxane was included in the third round of the Unregulated Contaminant Monitoring Rule (UCMR3) to evaluate its persistence in the environment and potential exposure to drinking water reservoirs. 1,4-Dioxane was detected in 21% of the 4864 public water systems monitored and exceeded the health-based reference concentration (0.35 µg/L) at 6.9% of these sites (Adamson et al., 2017). The EPA Integrated Risk Information System states that cancer development could occur in 1 out of 1,000,000 people exposed to a concentration of 0.35 ppb 1,4-Dioxane over a lifetime. Therefore, the UCMR3 is set to 0.07 µg/L for the United States.

Reliable evaluation of 1,4-Dioxane concentrations in the environment depend on analytical techniques for environmental sampling. Before the late 1990s, 1,4-Dioxane was often missed or overlooked during waste site characterization and remediation due to analytical limitations. More recent advances now permit detection at concentrations less

than 100 µg/L (Draper et al., 2000; EPA, 2008). Current data suggest 1,4-Dioxane is a frequent co-contaminant at Superfund sites and is generally found to be one of the most highly mobile contaminants on site (Zenker et al., 2003). A new understanding of 1,4-Dioxane presence in the environment has driven researchers to re-evaluate previously remediated sites with chlorinated legacy contaminants.

1,4-Dioxane concentrations in the environment vary greatly across the United States. Historical data (prior to 1990) suggests that ambient levels of 1,4-Dioxane in groundwater are about 1 µg/L (Kraybill, 1978). Approximately 6.9% of water supplies have 1,4-Dioxane levels above the MCL of 0.35 µg/L. The mean concentration is 1.1 µg/L for public water supplies (Adamson et al., 2017), but significantly higher levels have been found in various aquifers across the country. 1,4-Dioxane concentrations have been reported at 2,100 µg/L in Massachusetts (Burmaster, 1982), 31,000 µg/L in Westville, Indiana (Duwelius et al., 2002) and as high as 250,000 µg/L at a San Jose, California solvent recycling facility in 1998 (Gandesbery et al., 1998). Studies have shown that conventional wastewater treatment plants are often incapable of treating for 1,4-Dioxane, leading to discharge into surface waters (Simonich et al., 2013; Stepien et al., 2014).

1,4-Dioxane's low K_{OW}, K_{OC}, and Henry's Law constant (Table 1) illustrate that it is fully miscible in water and highly unlikely to retard or sorb to a solid phase. Further, 1,4-Dioxane is generally considered non-biodegradable. 1,4-Dioxane's infinite water solubility, negligible adsorption, and low volatilization (Table 1) have resulted in large

groundwater contaminant plumes. Due to these physiochemical properties, 1,4-Dioxane cannot be removed from groundwater through conventional treatment technologies, such as pump-and-treat or permanganate oxidation (DiGuiseppi and Whitesides, 2007). Consequently, 1,4-Dioxane has emerged as a recalcitrant groundwater contaminant across the United States (Abe, 1999; Jackson and Dwarakanath, 1999). Currently, *ex-situ* treatment of groundwater is the most common remediation method (DiGuiseppi and Whitesides, 2007; Mohr et al., 2016; Zenker et al., 2003), but this approach can be highly expensive and problematic with regards to disposing treated water and soils. Hence, alternative 1,4-Dioxane *in-situ* remediation strategies, such as advanced oxidation processes (AOPs), are being pursued. A promising *in-situ* treatment method is based on peroxone activated persulfate (PAP) oxidation of 1,4-Dioxane, which is an AOP proposed to degrade this contaminant through facilitated radical production (Eberle et al., 2016).

Molecular Mass (g/mol)	88.12
Log K_{ow}	0.43
Log K_{oc}	0.54
Vapor Pressure (mm Hg @ 25°C)	38.09
Henry's Constant (atm-m^3/mol)	$4.80*10^6$
Boiling Point (°C @ 760 mm Hg)	101.32

Table 1: Physiochemical properties of 1,4-Dioxane (DiGuiseppi and Whitesides, 2007; Mohr et al., 2016).

IN-SITU CHEMICAL OXIDATION (ISCO)

Compared to *ex-situ* treatment, *in-situ* chemical oxidation (ISCO) methods are desirable for their ability to treat groundwater without extraction. ISCO relies on the delivery of chemical oxidizing agents directly into the subsurface for the purpose of breaking down contaminants into less harmful chemical species (Huling and Pievetz, 2006). In general, chemical oxidation is the process of reducing an oxidant through accepting electrons released from the transformation of reactive species. Oxidation of targeted organic compounds is accomplished through hydrogen abstraction, oxygen addition, or electron removal. Commonly used ISCO oxidants include permanganate (MnO_4^-), hydrogen peroxide (H_2O_2), ozone (O_3), and activated persulfate ($S_20_8^-$) (Table 2) (Ferrarese et al., 2008; Rivas, 2006). The strength of an oxidant can be described in terms of oxidation and reduction potential (ORP). The ORP is a measure of a substance's ability at scavenging or donating electrons to another substance. The electrons that pass through these exchanges emit energy, which can be quantified as volts. The higher an oxidation potential, the stronger electron acceptor it is within an oxidizing system (Table 2).

Oxidant	Standard Oxidation Potential (Volts)
Hydroxyl Radical (•OH)	2.8
Sulfate Radical (•$S0_4$)	2.5
Ozone (O_3)	2.1
Persulfate (S_2O^{8-})	2.0
Hydrogen Peroxide (H_2O_2)	1.8
Perhydroxyl Radical (•HO_2)	1.7
Permanganate (MnO_4^-)	1.7
Chlorine (Cl^-)	1.4
Oxygen (O_2)	1.2
Hydroperoxide Anion (HO_2^-)	-0.9
Superoxide Radical (•O_2^-)	-2.4

Table 2: Oxidants and radical species with standard oxidation potential (Eberle et al., 2016; Huling and Pievetz, 2006; Siegrist, 2001).

Besides strength, another important factor to consider when choosing an oxidant is determining the reactive species' persistence in the environment (Table 5). Hydrogen peroxide and ozone are strong oxidants (1.8 V and 2.1 V, respectively), but they persist

for a maximum of several hours (P. A. Block et al., 2004; Huling and Pievetz, 2006). This is undesirable because short-lived oxidants cannot penetrate deeply into a polluted aquifer. Hence, oxidants that persist for days or weeks are preferred for ISCO applications.

While numerous pathways for oxidation exist, the primary goal is to transform targeted chemical pollutants into harmless byproducts. Once a groundwater plume is detected and characterized, oxidant solution is pumped into the ground via a network of strategically placed wells. The oxidant travels through treatment zones as a result of gravity and groundwater flow. The self-propagating dispersion of oxidant enables the oxidation of contaminants residing downgradient from the injection well(s) without need for groundwater extraction.

A multitude of reactants and conditions influence oxidation rates and pathways. Several researchers have demonstrated the successful degradation of 1,4-Dioxane with ozone (Brown et al., 2004; Suh and Mohseni, 2004); However, Suh and Mohseni (2004) found that the complete mineralization of 1,4-Dioxane into carbon dioxide was low, suggesting that organic intermediates were being formed. Their research also indicates organic intermediates are more readily degraded at an alkaline pH or in the presence of hydrogen peroxide.

While ISCO has been successfully applied to treat petroleum hydrocarbons, select chlorinated compounds, and other comparatively easy to oxidize compounds, this

approach has failed to break down more recalcitrant pollutants, such as per- and polyfluorinated substances, which require more advanced oxidant formulations.

ADVANCED OXIDATION PROCESSES (AOPS)

Advanced Oxidation Processes rely on the synergistic effects of combining strong oxidants for enhanced pollutant degradation in aqueous phase oxidation processes (Glaze and Wallace, 1984). Some of the strongest oxidants available are radicals. A radical, in chemistry, is a molecule that contains at least one unpaired electron. While many radical species can be used for remediation, commonly used radicals for *in-situ* and *ex-situ* chemical oxidation processes include hydroxyl (•OH) and or sulfate ($\bullet SO_4$) radicals. Depending on environmental parameters, radical formation may lead to further oxidation via secondary reactions, such as sulfate radical propagation.

In radical oxidation, oxidation rates depend largely on the quantity and type of radicals produced. Hydroxyl radicals can non-selectively oxidize most organic pollutants at very fast rates due to their high reactivity and oxidation potential (Buxton et al., 1988). Common •OH based AOPs include O_3, O_3/H_2O_2, UV/O_3, UV/H_2O_2, $UV/O_3/H_2O_2$, Fe^{2+}/H_2O_2, and electrolysis (Shen et al., 2017). However, hydroxyl radicals have a short lifetime (Table 3) which hinders the delivery of this oxidant to pockets of contaminant that are distant from the oxidant injection well(s). Hydroxyl radical production is a well-established mechanism for oxidizing 1,4-Dioxane (Adams et al., 1994; Bowman, 2001; McGrane, 1997; Stefan and Bolton, 1998; Zeng et al., 2017). The postulated destruction process includes primary oxidation through ozone.

Oxidant	Reactive Species	Reaction	Literature Referenced Persistence
Hydrogen Peroxide	Hydrogen Peroxide (H_2O_2)	$H_2O_2 + 2H^+ + 2e^- \rightarrow 2\ H_2O$	Minutes-hours
Ozone	Ozone (O_3) Hydroxyl radical (•OH)	$O_3 + 2H^+ + 2e^- \rightarrow O_2 + 2H_2O$ $2O_3 + 3H_2O \rightarrow 4O_2 + 2\ \bullet OH + 2H_2O$	Minutes-hours
Activated Persulfate ($S_2O_8^{2-}$)	Sulfate radical ($\bullet SO_4^-$) Hydroxyl radical (•OH)	$S_2O_8^{2-}$ + Peroxone $\rightarrow$ 2 $\bullet SO_4^{—}$ (initiation) $2\bullet SO_4^- + 2H_2O \rightarrow 2HSO_4^- + 2\ \bullet OH$ $2\ \bullet OH + 2H^+ + 2e^- \rightarrow 2\ H_2O$	Minutes-weeks

Table 3: OxyZone® reaction pathways (Ball, 2010; P. A. Block et al., 2004; Huling and Pievetz, 2006).

Hydrogen peroxide has a direct oxidation potential of 1.78 eV, but when catalyzed, peroxide forms •OH radicals with an oxidation potential of 2.78 eV (Table 4). The persulfate anion has a redox potential of 2.01 eV (Latimer, 1938). When activated,

persulfate is capable of producing both hydroxyl and sulfate radicals (Block et al., 2004; Huling and Pievetz, 2006). The $\bullet SO_4$ radical has redox potential of 2.6 V (Table 4).

Primary Oxidation via Ozone	$O_3 + 2H^+ + 2e^- \rightarrow O_2 + H_2O$
Hydroxyl Radical Formation	$O_3 + H_2O \rightarrow O_2 + 2\bullet OH$ $2O_3 + 3H_2O_2 \rightarrow 4O_2 + 2\bullet OH + 2\ H_2O$
Oxidation by Hydroxyl Radical	$2\bullet OH + 2H^+ + 2e^- \rightarrow 2H_2O$
Primary Oxidation via Persulfate	$S_2O_8^{-2} + 2H^+ + 2e^- \rightarrow 2HSO_4^{-1}$
Hydroxyl and Sulfate Radical Formation	$S_2O_8^{2-} + H_2O_2 \rightarrow 2\bullet SO_4^- + 2\bullet OH$
Oxidation by Hydroxyl Radical	$2\bullet OH + 2H^+ + 2e^- \rightarrow 2H_2O$
Oxidation by Sulfate Radical	$\bullet SO_4^- + e^- \rightarrow SO_4^{2-}$

Table 4: OxyZone® reaction pathways (Block et al., 2004; Eberle et al., 2016; Huling and Pievetz, 2006).

Ozone, under the right conditions, can yield hydroxyl radicals, which have the ability to self-propagate. Ozone oxidation yields the hydroxyl radical, a stronger (2.78 eV) but short-lived oxidant. Activated sodium persulfate can yield both hydroxyl and sulfate

radicals. The sulfate radical is slightly lower in electrode potential (2.1 V), but has the ability to persist for weeks (Ball, 2010).

Activated sodium persulfate is capable of producing both hydroxyl and sulfate radicals (P. a Block et al., 2004; Huling and Pievetz, 2006). Persulfate can be activated by UV light (He et al., 2014; Tsitonaki et al., 2010), heat (Liang et al., 2003), alkaline base (Furman et al., 2010) or iron (P. a Block et al., 2004; Crimi and Taylor, 2007), or by hydrogen peroxide and ozone, known as peroxone activation. Peroxone activated persulfate (PAP) is a promising AOP technology due to the stability of the sulfate radical, which permits the oxidant to travel further when injected into the subsurface (Huling and Pievetz, 2006; ITRC, 2005; SERDP, 2011).

One particular peroxone oxidant formulation that has been recently introduced is OxyZone® (U.S. patent No. 7,667,087). Developed by EnChem Engineering (Newton, MA), OxyZone is a peroxone activated persulfate based AOP technology. OxyZone uses a blend of ozone, sodium persulfate, phosphate buffers, and hydrogen peroxide and is used predominantly for the in-situ treatment of organic compounds, such as gasoline, fuel oils, and chlorinated volatile organic compounds (Ball, 2010). It is assumed that the presence of ozone and hydrogen peroxide in the persulfanated oxidant mix results in the production of hydroxyl (•OH) and sulfate ($\bullet SO_4^-$) radicals (Table 4) (Block et al., 2004; Crimi and Taylor, 2007; Furman et al., 2010; Peyton, 1993). The production of these radicals is attributed to the breaking-down of organic contaminants. Further, a decrease in pH during oxidation is well documented in this and other activated persulfate-oxidant

systems (Block et al., 2004; Eberle et al., 2016; Huang et al., 2005, 2002, Liang et al., 2003, 2011; Waisner et al., 2008). In general, activated persulfate oxidants are a promising group of in-situ chemical oxidation technologies (ITRC, 2005; SERDP, 2011), but knowledge gaps exist regarding the treatment of 1,4-Dioxane.

Prior studies conducted at the University of Rhode Island demonstrated that OxyZone is capable of destroying 1,4-Dioxane, together with its co-contaminants, namely 1,1,1-TCA and TCE (Eberle et al., 2016). These studies also showed continued oxidation of organic contaminants with OxyZone up to 96 hours (Eberle, 2015). OxyZone's capability for persistent oxidation suggests that radicals are formed during the oxidation process, and continue to drive the reactions. Further, Eberle et al. (2016) found that the rate of oxidation for each contaminant increased linearly with increasing persulfate concentration. The destruction process was described by pseudo first-order reaction kinetics when conducted in aqueous batch solutions (Eberle, 2015); however, these prior bench-scale tests were carried out in aqueous phase only, i.e. the possible effect of aquifer solids on the reaction rate in the pore water was not investigated. The formation of radicals during OxyZone reactions was postulated by Eberle (2015) based on significantly elevated oxidation reduction potential (ORP >900 mV) and drop of pH during treatment. While an elevated ORP strongly suggests radical formation, Dr. Eberle's work did not identify the exact reactive species produced during the reaction.

The formation of radicals can be studied with a spectroscopy technique known as *Electron Paramagnetic Resonance* (EPR). EPR captures the intensity and frequency of unpaired electron movement between oscillating magnetic poles as they emit or absorb a photon of energy (hv) while moving between energy levels. EPR identifies electrons with orbital and spin angular momentum. The chemical shift between the two momentums is scaled to account for coupling, which is known as the Lande g-factor or the g-factor. EPR quantifies spin angular momentum to define a spin state. Unpaired electrons orient themselves parallel to a large magnetic field. This process causes Zeeman splitting where the energy difference between the energy levels matches the microwave frequency. The spectrometer records the absorption of energy from Zeeman splitting. Radical species are identified by the change in g-factor (Δg).

Combined with spin trapping, EPR spectroscopy can identify free radicals. Spin trapping agents react covalently with radical products to form more stable adduct for detectable paramagnetic resonance spectra (Janzen, 1965). This is, free radicals cannot be observed at room temperature due to short spin relaxation times (Basumallick et al., 2009). A spin trap stabilizes the radical adducts in order to be detected using EPR. The spin-trap 5,5-dimethyl-1-pyrroline-N-oxide (DMPO) ($C_6H_{11}NO$) is a commonly used chemical to capture EPR spectra (Figure 3). Spin traps are diamagnetic radical scavengers that scavenge reactive free radicals to produce an EPR signal (Harbour et al., 1974) (Figure 3). The letter “R” (Figure 3) represents any radical species produced in the reaction process. The nitrogen located at the base of the DMPO is responsible for

forming nitroxides. Spin traps such as DMPO scavenge the •OH radicals produced during oxidation and produce a characteristic nitroxide which is detectable through EPR (Jaeger and Bard, 1979). DMPO forms radical adducts in C, N, S, and O-centered radicals and produces distinguishable EPR spectra. Determining the exact radical species is done by identifying hyperfine splitting of the spin adducts through published scientific literature (Table 5). Because pure quartz does not bear detectable surface radicals or other paramagnetic centers, as indicated by the absence of any EPR spectrum (Fubini et al., 1989), there is no concern for radical interaction or interference with quartz sand.

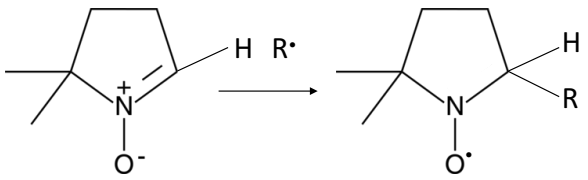

Figure 3: DMPO molecule and DMPO radical R adduct. DMPO has a molecular mass of 113.2 grams/mole.

Adduct	α_N	$\alpha^{\beta}{}_H$	$\alpha^{\gamma 1}{}_H$	$\alpha^{\gamma 2}{}_H$
•HO	14.9	14.9	N/A	N/A

$\bullet SO_4^-$	13.7	10.1	1.42	0.75

Table 5: Hyperfine coupling constant values using DMPO spin adducts (Cheng et al., 2003; Fang et al., 2013; Furman et al., 2010; Mottley and Mason, 1988; Yan et al., 2015).

Spin trapping combined with EPR spectroscopy will be used to study the radicals involved in the peroxone activated persulfate reaction with 1,4-Dioxane. Previously, this approach has successfully identified radical production during the oxidation of 1,4-Dioxane using Fenton's Reagent (Zhong et al., 2015). However, this research project is the first documented application of EPR to identify radial species produced during the peroxone activated persulfate treatment of 1,4-Dioxane using OxyZone®.

1.2 Objectives

The principal objective of this study was to investigate the degradation of 1,4-Dioxane through oxidation with OxyZone® under dynamic, flow through conditions that mimic the *in-situ* treatment of groundwater plumes. Batch experiments will be conducted to determine 1,4-Dioxane degradation rates in the presence of homogenous quartz sand under static conditions. Two different oxidant injection schemes were studied, i.e. slug injection into one or two "wells", respectively. Non-reactive tracer tests characterized the physical transport behavior of the oxidant and the hydraulics of the experimental system. The reaction rates of 1,4-Dioxane oxidation with OxyZone in the presence of sediment were used to make projections for OxyZone use at contaminated field sites. This study's secondary objective was to identify the radicals produced during

oxidation of 1,4-Dioxane water with OxyZone. Based on the chemical composition of OxyZone, it is hypothesized that both hydroxyl and sulfate radicals are produced. The data presented herein addresses some of the current knowledge gaps regarding the treatment of 1,4-Dioxane. The findings will be useful for the planning and future testing of 1,4-Dioxane *in-situ* treatment schemes under pilot- or field-scale conditions.

METHODS

2.1 MATERIALS AND ANALYTICAL METHODS

1,4-Dioxane (Figure 1) was obtained from ACROS (99.5% purity). Unless stated otherwise, all other chemicals were purchased from Fisher Scientific, including sodium persulfate ($Na_2O_8S_2$, >98% purity), sodium phosphate dibasic anhydrous (HNa_2O_4P, >99% purity), hydrogen peroxide (H_2O_2, 30% solution) and sodium thiosulfate pentahydrate solution (1N, $Na_2S_2O_3 \cdot 5H_2O$). Ozone was generated with a Pacific Ozone L11 Ozone Generator with ultra-high purity oxygen (Airgas, OX300). 1,4-Dioxane and deuterated 1,4-Dioxane-d8 standards were obtained from SPEX CertiPrep. Analytical samples were diluted in purge-and-trap grade methanol (99.9+% purity) whereas ACS grade methanol (99.8% purity) was used for cleaning equipment.

Homogenous silica quartz Accusand sand (2mm mesh size #10) was purchased from Unimin Corporation, Le Suer, MN. Accusand is a well-characterized porous media used to standardize the efficiency of laboratory flow experiments (Schroth et al., 1996).

ORP and pH were measured with a Hach HQd11d Portable Starter MTC101 ORP electrode from Cole-Parmer.

OxyZone® Generation: OxyZone is a patented peroxone activated buffered persulfate solution (Ball, 2010) that is commercialized by EnChem Engineering INC, (Newton, MA). OxyZone is generated by saturating a phosphate-buffered persulfate solution containing hydrogen peroxide with ozone at ambient temperatures. The oxidant was produced in a semi-batch reactor provided by EnChem Engineering. The batch reactor is designed to ozonate 3.5 L of liquid. After 25 minutes of pumping ozone gas through the reactor, gas flow was halted and the oxidant solution was drawn from the reactor for immediate use. The molar concentration of full-strength OxyZone is 0.252 moles/L with respect to sodium persulfate. Table 6 shows the physical properties of OxyZone.

Molar Concentration (moles/liter)	ORP (mV)	EC (µS/cm)	pH
0.252	612	4130	4.4

Table 6: Physical properties of OxyZone.

Analytical: 1,4-Dioxane concentrations were analyzed with a gas chromatograph mass spectrometer from Shimadzu (GCMS-QP2010SE) equipped with a Restek Rxi®-624Sil MS column (30 m, 0.25 mm ID, 1.4 µm). Aqueous samples were introduced through an OI Analytical Eclipse 4660 Purge and Trap sample connector equipped with a #7 Tenax trap

and a 25 mL sparging vessel. Samples were analyzed with ultra-pure helium gas (AirGas). Analysis of 1,4-Dioxane was performed in selected ion monitoring (SIM) mode. 1,4-Dioxane and an internal standard of deuterated 1,4-Dioxane-d8 was used to correct for purge accuracy variation. The following equation (Eqn 1) was used for sample correction:

$$C_a = C_i \times (M_a/M_i) \qquad \text{Eqn 1}$$

Where C_a is the estimated concentration of the target analyte, C_i is the known concentration of internal standard added, M_a is the target analyte's measured concentration, and M_i is the internal standard's measured concentration. Internal Standard 1,4-Dioxane-d8 recovery must fall into 60-140% recovery to be accepted for statistical analysis. Samples with an internal standard recovery outside of these parameters were re-run until recovery fell into the accepted range.

2.2 Batch Scale Methods

Bench scale experiments were conducted to determine destruction rates of 1,4-Dioxane exposed to OxyZone® in the presence of homogenous silica quartz sand (2mm Mesh size #10, Accusand®) through batch scale experiments. For the initial set of experiments, OxyZone® and 1,4-Dioxane concentrations were adjusted to oxidant-to-contaminant molar ratio previously used by Eberle (2016). Amber glass vials typically used for volatile organic analysis with Teflon seals (40 mL VOA, Fisher Scientific) were filled with 20g (dry weight) of homogenized quartz sand (2mm, Mesh Size 10, Accusand).

Contaminant-solutions were prepared from stock solutions of 3533 µg/L +/- 249.84 µg/L 1,4-Dioxane. Each vial was filled with 3.25 mL of 1,4-Dioxane. OxyZone was diluted with Deionized water to prepare solutions with molar oxidant: contaminant ratios ranging from 0:1, 100:1, 250:1, 500:1, to 1000:1. Each VOA vial was completely filled with their respective oxidant: contaminant solution to eliminate headspace and agitated at 25°C for 24 hours. After 24 hours of reaction time, all solutions were transferred to 20mL VOA vials containing 1N sodium thiosulfate to quench the reactions. The vials were refrigerated at 4°C until analysis. For quality assurance, triplicate samples were taken for each oxidant: contaminant ratio. Control triplicates, containing 1,4-Dioxane but no oxidant, were prepared and analyzed.

For elucidating the degradation kinetics of 1,4-Dioxane oxidation in the presence of sand, a second bench scale test was conducted using a constant oxidant: contaminant molar ratio of 250:1. At this ratio, the reaction was sufficiently slow to ensure that 1,4-Dioxane was measurable over the entire test duration (16 days). As before, 20g of sand in amber 40mL VOA vials was spiked with 3.25mL of 1,4-Dioxane solution (C_o=3533 µg/L +/- 249.84 µg/L). The remaining space was filled with a solution containing a 250:1 molar ratio of oxidant: contaminant. Samples were agitated at 25° C at the rate of 4 rotations per minute. At different times, samples were transferred to 20mL VOA vials and quenched 3mL 1N sodium thiosulfate. The time points were 0 hours, 2 hours, 8 hours, 24 hours, 2 days, 4 days, 8 days, and 16 days. Triplicate samples were taken at each time for quality assurance. After analysis, chemical kinetics were analyzed. Due to a great excess

of sodium persulfate in the AOP system, relative to 1,4-Dioxane, its concentration remains relatively constant throughout the duration of reactions. Therefore, the reactions taking place are considered to be pseudo-first order. By plotting the natural log of (C/C_o) versus time, the slope of the line equals the rate constant of the overall reaction:

$$-d[\frac{\frac{C}{Co}}{dt}] = k[\frac{C}{Co}] \quad \text{Eqn 2}$$

Once the rate constant, k, is determined, the half-life , $t_{½}$, can be calculated (Capellos and Bielski, 1972).

$$t(\frac{1}{2}) = \frac{1}{k[\frac{C}{Co}]} \quad \text{Eqn 3}$$

2.3 Column Tests

A custom-made column was used to conduct column-scale tests of 1,4-Dioxane degradation by OxyZone under conditions mimicking *in-situ* AOP treatment. The column was constructed from a 152.4 cm section of clear polyvinyl chloride pipe with 7.73 cm in diameter (Everclear PVC) (Figure 4). Teflon tape lined PVC caps were threaded on each end. The column was outfitted with five stainless steel septa ports (Swagelok) for sample collection or oxidant injection (Ports A through E). Three additional ports were installed for inserting GS3 Greenhouse Sensor Probes (Decagon) (Probes 1 through 3; Figure 4). Each probe was connected to an EM50 EC Data Logger (EM25312, Decagon) to store electrical conductivity (EC), soil moisture, and temperature readings at five-minute intervals. The column was packed with homogenous quartz sand (2mm mesh size #10,

Accusand®). A layer of clean glass wool was inserted before capping the column to prevent headspace and the escape of sand particles. The caps on both ends of the column were fitted with stainless steel compressional tube adopters (Swagelok). The column was mounted vertically to the wall. The inlet at the bottom of the column was connected with 3/8" Teflon tubing (TYGON) leading to a peristaltic pump (Cole-Parmer Gear Pump System RN-74013-70). The column outlet on the top was also connected to 3/8" Teflon tubing, leading to the sample collection station. The dimensions of the column, including the amount of sand it contained, are summarized in Table 7.

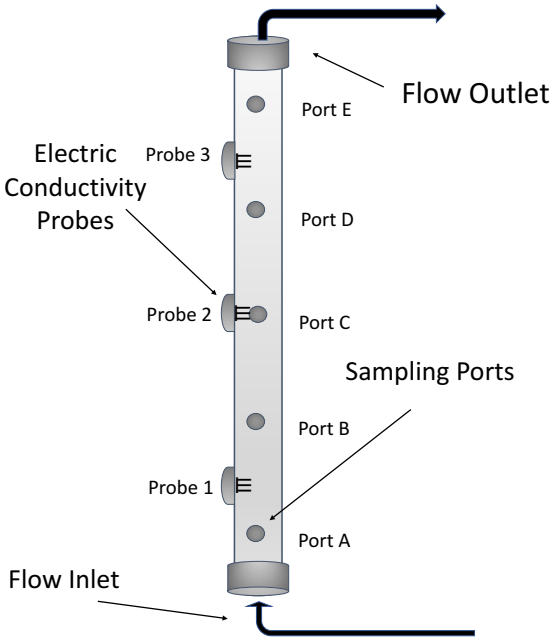

Figure 4: Schematic of column used for flow through experiments. The column is 152.4 cm length, 7.73 cm diameter.

Length (cm)	Diameter (cm)	Area (cm^2)	Volume (cm^3)	Weight Empty Column (g)	Weight Packed Column (g)	Weight Sand (g)	Weight Water Saturated column (g)	Weight water (g)	Porosity (%)
152.4	7.73	46.9	7,148.5	5,780	11,530	5,750	13,600	2,070	29

Table 7: Properties of packed column.

After packing the column with sand, deionized water was pumped at a rate of 4.1 mL/minute upwards through the column for several days, i.e. until effluent EC readings were similar to the influent (10 µS/cm) and until all entrapped air exited the column. This was determined by monitoring the moisture content at each probe. Once saturated, the weight of the column was determined and the porosity of the sand calculated from the difference of the weight of the dry and saturated sand (Table 7). The porosity was 29%, which is concurrent with the values reported for characterized Accusand (Schroth et al., 1996). In absolute terms, the volume of water inside the column represents 2070 cm^3 of the bulk volume of the column (7148.5 cm^3). For both tests, the column was saturated with 300 µg/L 1,4-Dioxane (3 mM/L). This set the oxidant: contaminant ratio for all studies at 7,400:1. This ratio is an estimate due to the dynamic flow conditions of the column.

Conservative Tracer Test: A conservative tracer test was conducted to characterize the column hydraulics. A conservative tracer, e.g. sodium chloride (NaCl), is not expected to interact with the experimental matrix, such as the sand or the column material. 210 mL NaCl solution (2,000 mg/L, ACS reagent, ≥ 99%) was flushed through the column at the

constant rate of 4.26 mL/min, followed by deionized water injection. EC readings were logged at Ports 1 through 3 every five minutes. EC measurement of column effluent samples were taken in 16-minute intervals. The EC readings were converted to NaCl concentration via a calibration line (R^2= 0.998) (Appendix x1). The NaCl concentrations were then transformed into dimensionless concentrations, $C/C_{o,}$ where C_o is the initial NaCl concentration and C is the concentration measured at each time step. The data was plotted versus pore volume (PV) to determine the tracer transport through the column (Figure 7). Pore volumes, U, is dimensionless time, defined as:

$$U = \frac{V_x nAt}{ALn} = \frac{Qt}{ALn} = \frac{V_x t}{L} = t_R \qquad \text{Eqn 4}$$

Where V_x is the linear velocity, n is porosity, A is area, L is the length of the column, Q is the discharge, and t_R is relative time (Brigham, 1974). By converting to dimensionless units, it is possible to directly compare data from different tests and varying test conditions. The graph of concentration versus time is known as a breakthrough curve. Important characteristics of the breakthrough curve include the tracer arrival time, which is equivalent to the flow velocity of the water inside the column, the arrival of the tracer's center of mass, tracer mass recovery, and information about tracer pulse dispersion. The corresponding data can be quantified using the Method of Moments (Fetter et al., 2017).

Contamination Procedure: The Agency for Toxic Substances and Disease Registry (ATSDR) screening level for 1,4-Dioxane based on the EPA IRIS Reference Dose (US EPA, 2011) is set at 300 µg/L. This risk level was chosen as the starting concentration for all experiments. A solution of 300 µg/L 1,4-Dioxane in water (was pumped into the column until the effluent concentration was at equilibrium with the influent one. The pump rate was a constant 4.26 mL/min. Equilibrium was achieved after 36 hours.

2.4 AOP Treatment of 1,4-Dioxane with OxyZone

Two treatment scenarios were evaluated. First, two slugs of equal volume (100mL each) of OxyZone were injected at two ports into the 1,4-Dioxane contaminated sand-packed column. Second, one slug of 200mL OxyZone (equal in volume of the two slugs of the first test combined) was injected at the bottom of the column. During both tests, the rate of discharge flow was Q=4.1 mL/min and the specific discharge (v=Q/A) was 0.13 cm/min. The slugs were injected into 1,4-Dioxane contaminated water moving at an average linear velocity of 0.45 cm/min, which is about an order of magnitude higher than typical flow rates of groundwater plumes at contaminated sites. During all experiments, the following parameters were monitored: EC, ORP, pH, temperature, 1,4-Dioxane concentration. The persulfate concentration was monitored indirectly by EC proxy for persulfate during the first test scenario. That is, the EC of OxyZone is approximately 41 mS/cm, whereas that of 1,4-Dioxane is $2*10^{-3}$ mS/cm. Assuming that the great excess of

persulfate and the resulting high EC does not change measurably during the test, EC can be used as a proxy for oxidant transport throughout the column.

TREATMENT SCENARIO I - SLUG INJECTION IN TWO PORTS:

Slugs of 100 mL OxyZone were simultaneously injected into Ports A and C (Figure 4) at a rate of about 4 mL/minute, using gas-tight Duran syringes (total duration of injection: 25 min). Each syringe was equipped with a stainless steel 6" leur-lock needle (Thermo Scientific). The longer needles allowed for OxyZone to be injected directly into the center of the packed column. Effluent samples were continuously collected in 15 minute intervals over the duration of the experiment (10 hrs). Each effluent sample, approximately 60 mL, was aliquoted into two samples (three when taking duplicates). The first aliquot was consumed for measuring pH, ORP, and electric conductivity. The second sample was quenched with 1N sodium thiosulfate and refrigerated at 4°C until 1,4-Dioxane analysis. For quality control, a replicate sample was collected at every 9th time point. A second test of treatment scenario I was conducted, following the same procedure except that OxyZone was injected at half the rate (2 mL/minute) for 50 minutes to obtain a greater mixing and dispersion.

TREATMENT SCENARIO II – SINGLE SLUG INJECTION:

One slug of 200 mL OxyZone was injected at the bottom of the column at a rate of 13 mL/min (total duration of injection: 15.5 minutes). The sampling and analysis procedures were identical to Treatment Scenario I procedures.

2.5 Electron Paramagnetic Resonance

Electron Paramagnetic Resonance (EPR) was used to study radical formation. All samples were analyzed with a Bruker® EMX Model EPR, operating at the parameters described in Table 8. Methods developed by Zhong et al. (2015) were used to analyze radical formation. Spin trap DMPO-OH (5,5-Dimethyl-1-Pyrroline-N-Oxide) was purchased from Cayman Chemical, Ann Arbor, MI and used as received. DMPO-OH was frozen and stored at -4°C before use. The energy required for the activation of molecules in aqueous solution was provided by ultraviolet light, except for studying OxyZone solutions, which were activated by peroxone.

EPR spectra were obtained for all components that make-up OxyZone, including all possible combinations of OxyZone constituents with and without the presence of 1,4-Dioxane (Appendix C4-C23). An EPR spectra library was put together to determine which radical(s) were produced by what compound or mixtures of compounds.

A solution containing 5 mM DMPO along with a mixture of varying OxyZone constituents were prepared in batches. All experiments were modeled after Zhong (2015) and used a target concentration of 5 mM sodium persulfate and 0.5mM 1,4-Dioxane. For

EPR runs, 200 µL of solution was injected into micro-Teflon tubing and immediately submerged in liquid nitrogen to retard reactions. Each sample was inserted into a standard quartz cuvette with 1 mm path length. All samples were activated using a UV light and focused with a quartz lens. Multiple replicates of each sample were analyzed. All measurements were taken at room temperature. Data acquisition and processing was achieved with Bruker's ESP software, WinEPR. Each EPR spectra represents 100 averaged scans. Peaks were identified using published literature.

Prior studies show that •OH and $•HO_2$ radicals are intermediates generated from hydrogen peroxide under UV photolysis (Czapski and Bielski, 1963; Wyard et al., 1968). Hydrogen peroxide, sodium persulfate, and 1,4-Dioxane are weak absorbers of UV light. Therefore, no direct photolysis of 1,4-Dioxane is expected. Using DMPO-OH as an adduct gives α_H and α_N identical values of 14.9, which gives the intensity ratio of 1:2:2:1 (Table 6).

Field	
Center Field (G)	3480.000
Sweep Width (G)	150.000
Resolution (points)	1024
Microwave	
Frequency (GHz)	9.805
Power (mW)	20.850
Receiver	
Receiver Gain	2.52e+004
Phase (deg)	0.00
Harmonic	1
Mod. Frequency (kHz)	100.00
Mod. Amplitude (G)	1.00
Signal Channel	
Conversion (ms)	40.960
Time Constant (ms)	1.280
Sweep Time (s)	41.943

Table 8: EPR parameters used for all spin-trapping experiments.

RESULTS

3.1 Batch Scale Experiments

Batch scale experiments were used to determine the degradation of 1,4-Dioxane using OxyZone in the presence of homogenized silica quartz sand under varying oxidant:

contaminant ratios, derive reaction kinetics, and compare the results with those of Eberle (2016), who studied aqueous phase kinetics in the absence of sediment.

The first set of batch studies covered oxidant: contaminant (OxyZone to 1,4-Dioxane) molar ratios ranging from 100:1, 250:1, 500:1, and 1000:1 and lasted 24 hours (Appendix Table C1). The experiment was carried out to determine the optimal oxidant: contaminant ratio for the subsequent kinetics study. Figure C1 indicates that at high ratios (≥500:1), 1,4-Dioxane is comparatively quickly destroyed. At 250:1 or lower, 1,4-Dioxane destruction is sufficiently slow to monitor it over an extended period, i.e. about two weeks. Based on these results, a 250:1 ratio was chosen to conduct the following kinetics study. For comparison, the initial OxyZone oxidant: contaminant ratio is 7,400:1 before it is being injected into the column or injected into a polluted aquifer under field test conditions.

The second set of batch experiments kept the oxidant: contaminant ratio fixed at 250:1 but extended the reaction period to 16 days (Figure 5). The control experiment proved that no significant degradation took place in the absence of oxidant, whereas the 1,4-Dioxane concentration dropped to below detection limit when exposed to oxidant after 192 hours (Figure 5). By plotting the relative concentrations at each time point (Figure 6) and using the slope of the best-fit line for solving Eqns. 2 and 3, the reaction rate and half-life time was determined (Table 9).

k_1 (h^{-1})	0.0213
$T_{1/2}$ (h)	33
R^2	0.97

Table 9: Oxidation of 1,4-Dioxane over 16 days (384 hours) at the oxidant: contaminant ratio of 250:1.

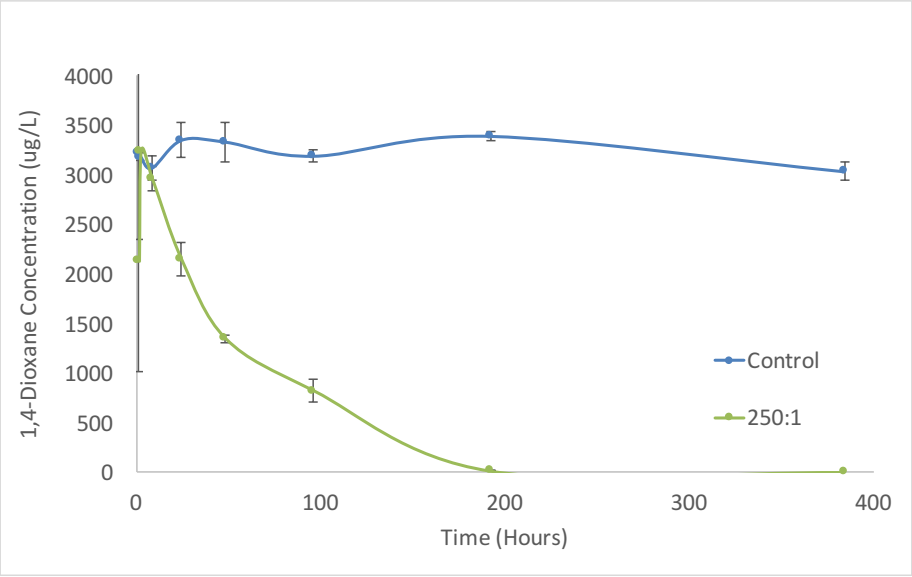

Figure 5: Batch scale oxidation of 1,4-Dioxane over time oxidant: contaminant ratio of 250:1.

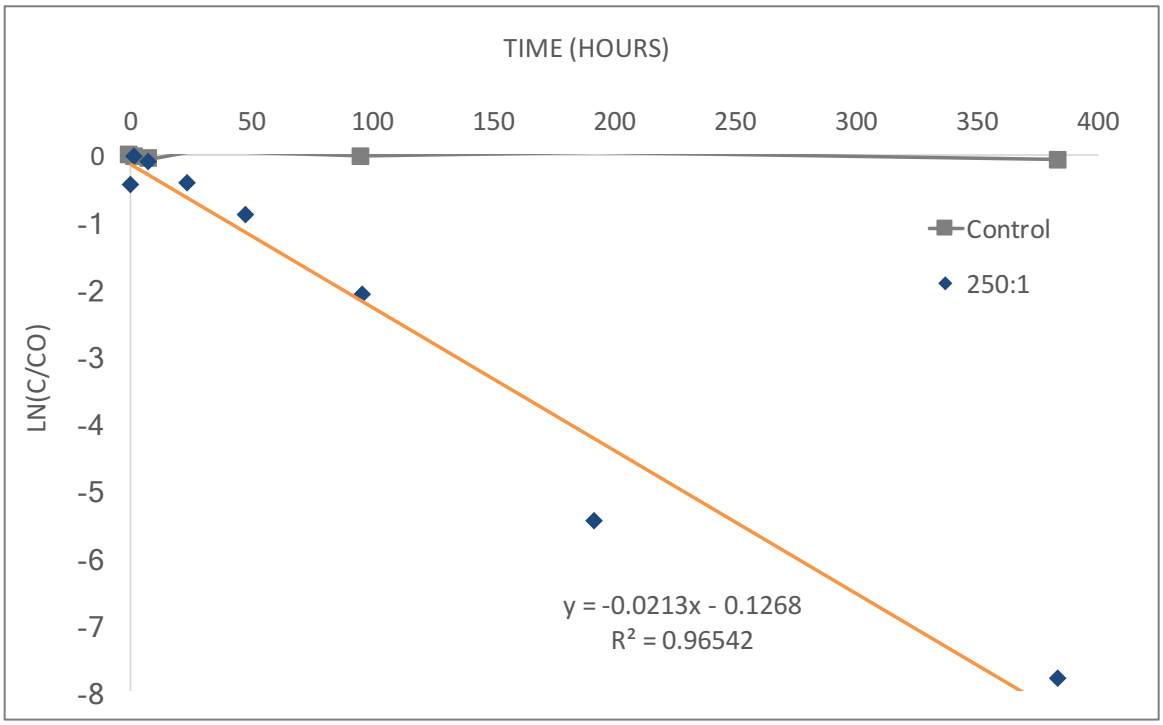

Figure 6: Ln(C/Co) over time for the 16-day period at the oxidant: contaminant ratio 250:1.

3.2 Column Experiments

Column scale tests were conducted to obtain an understanding of 1,4-Dioxane treatment under dynamic, flow through conditions. An initial conservative tracer test indicates that the column is packed homogenously and that preferential flow is negligible. The tracer breakthrough curve followed a Gaussian distribution and the arrival of the tracer front was observed with minor delay (1.09 PV), and dispersion was minimal (±0.08 PV) (Figure 7). However, for reasons unknown the tracer mass recovery was 20% higher than expected.

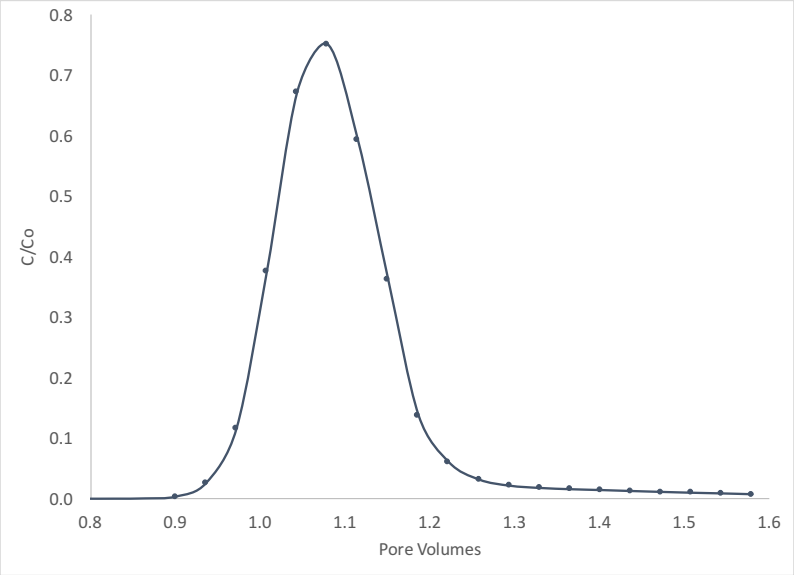

Figure 7: Conservative tracer breakthrough curve.

M_O	M_1 (PV)	M_2 (PV)
120%	1.09	±0.08

Table 10: Temporal moment analysis for sodium chloride conservative tracer test.

TREATMENT SCENARIO I - SLUG INJECTION IN TWO PORTS

Two tests were conducted under this scenario, differing only in the time it took to inject 100 mL (about 0.05 PV) slugs of oxidant each into two ports (A and C; Figure 4). During the first test (Test I), the oxidant was injected quickly, i.e. within 25 minutes. The test ran for 12 hours or just under 1.5 pore volumes. There are two peaks in the EC data, at 0.55 PV and 0.95 PV respectively, which signal the breakthrough of the two separate slugs (Figure 8). Inflow 1,4-Dioxane concentration was 268 µg/L. At 0.4 PV, the concentration rose to 376 µg/L (Figure 8). This anomaly is also reflected in the ORP and

pH data (Figure 9). Following the breakthrough of the oxidant, as indicated by the rise in EC, the ORP values rose to 276.5 mV, while 1,4-Dioxane concentration decreased (to as low as 215 µg/L, or 0.55 C/Co). The pH decline appears inversely related to the rise in ORP (Figure 9). The pH of the system starts at near neutral and eventually stabilizes at around 6.4.

The M_0 moment describes the oxidant mass recovery. For Scenario I, Test I, only 7.66 grams of OxyZone was recovered in the effluent, or 51% of the total mass injected. However, the EC readings were elevated still at the end of the experiment (Figure 8), indicating that an unknown fraction of the oxidant had not eluted from the column.

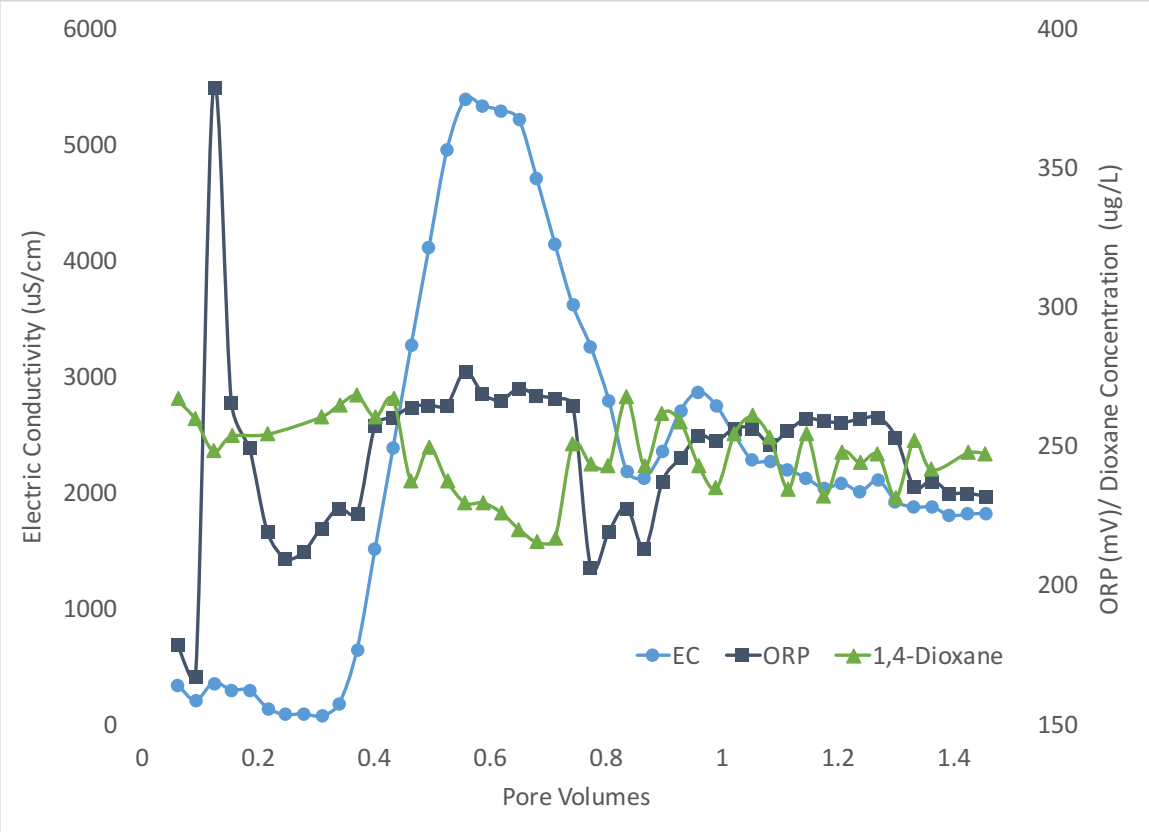

Figure 8: Results from Scenario I Test I experiments, ORP, EC, and 1,4-Dioxane concentration.

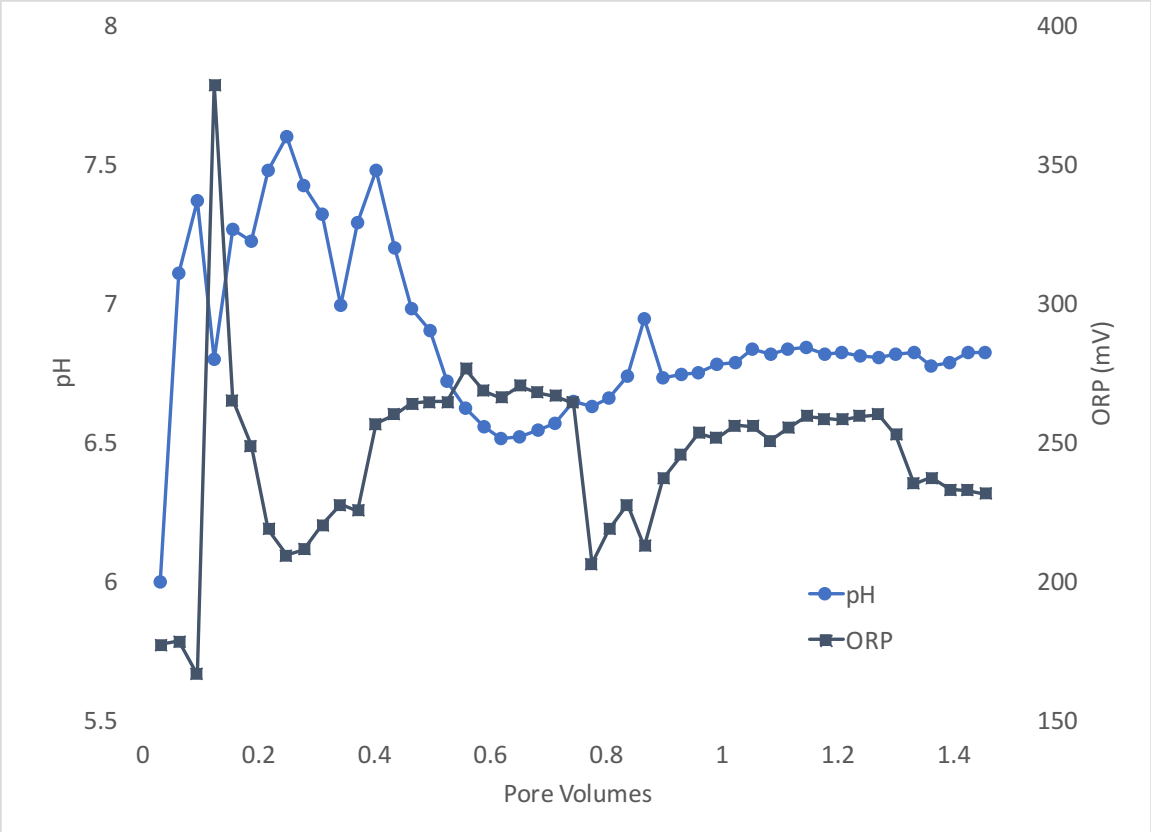

Figure 9: Results from Scenario I Test I experiments, pH and ORP.

Based on the 1,4-Dioxane concentration data during the breakthrough of the first slug of oxidant solution (pore volumes 0.4 to 0.7), the 1,4-Dioxane degradation rate was calculated (k= 0.08 h^{-1}; Figure 10). The breakthrough of the second slug had no distinct effect on the 1,4-Dioxane concentration and therefore no rate was calculated from this data set.

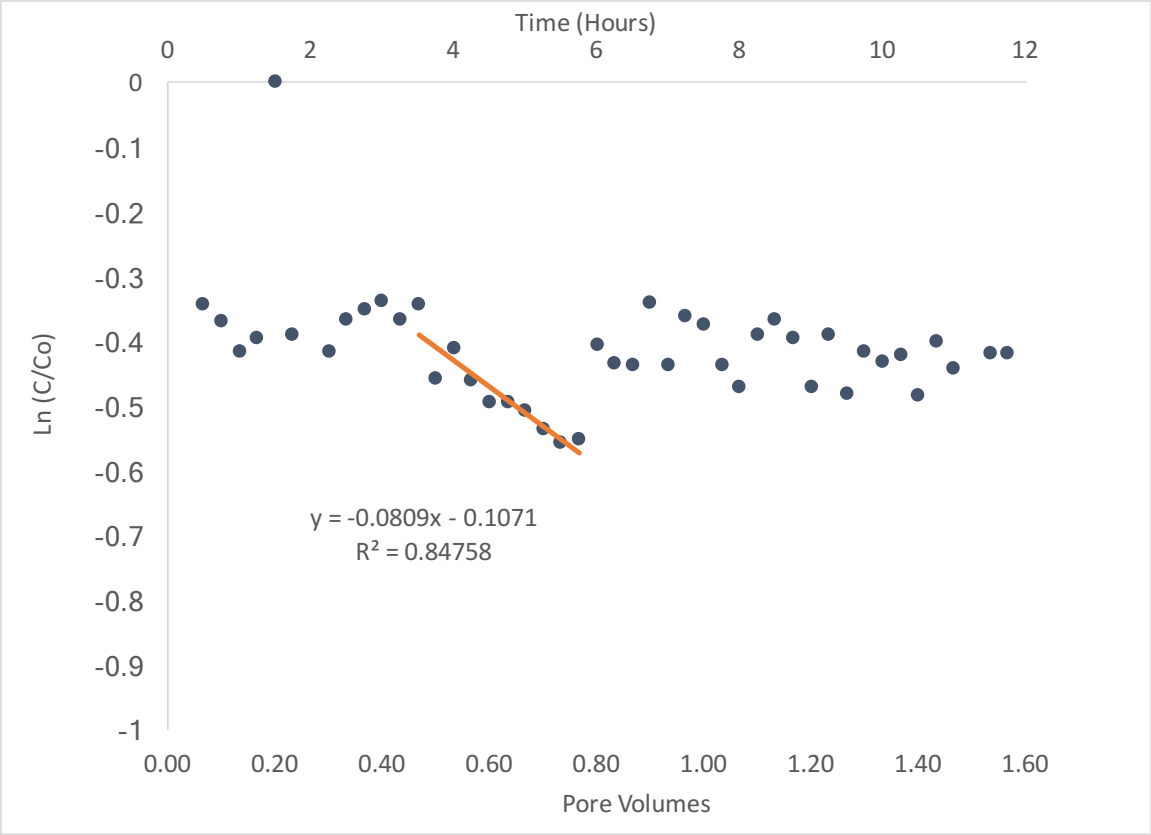

Figure 10: Scenario I, Test 1: The 1,4-Dioxane degradation rate was calculated as k= 0.08 h^{-1}.

During the second trial of scenario I (Test II), experimental conditions were identical to Test I with the exception that the oxidant injection time was twice as long (50 min). The experiment continued for 16 hours, or about 2 pore volumes. As for Test I, the pH falls from initially 7.0 to between 6.0 and 6.5 while the ORP rises from less than 240 to maximal 443 mV (Figure 11). Interestingly, also as before, there is a distinct anomaly

shortly after oxidant injection, i.e. pore volume 0.2, where pH sharply drops to <5.0 and ORP sharply rises to 475 mV. Both then return to near-base values.

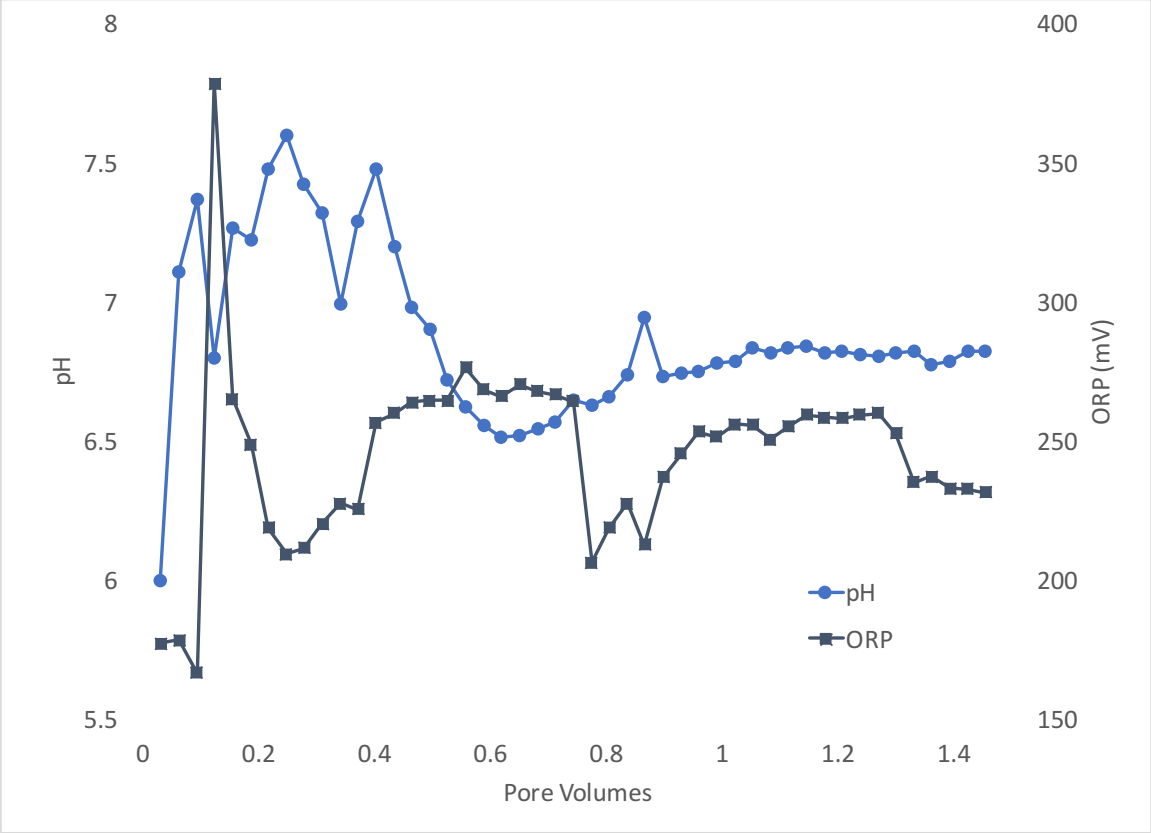

Figure 11: Results from Scenario I Test II experiments, pH and ORP.

Figure 12 shows the 1,4-Dioxane column effluent concentrations, which, for comparison, was plotted against ORP and EC. The EC peaks at 0.58 PV and 0.96 PV at respective values of 2990 µS/cm and 5230 µS/cm. These peaks clearly reflect the breakthrough of two slugs. The EC peak value of the second slug, breaking through at a

later time, is about twice as high as the earlier peak, suggesting that some overlap of the two slugs has occurred. Even at the end of the experiment, i.e. after 2 PV, the EC did not return to the initial 0.3 µS/cm. A similar behavior was observed for the ORP data, which remained high even after the oxidant should have completely left the column system if behaving as a conservative solute. This indicates that some of the oxidant remained behind in the column, only slowly leaching out. This assessment is corroborated by the zeroth moment (M_0) which shows an oxidant mass recovery of 10.26 g, or 76% (Table C3).

It is noted that the breakthrough of the second oxidant slug did not result in much higher ORP readings, i.e. unlike EC, the ORP is not additive in case slugs overlap. The 1,4-Dioxane concentration decreased from 302 µg/L to 188 µg/L, (C/Co=0.62), when ORP and EC were at their respective maximum values at about 1 PV. Even after 1,4-Dioxane concentration rose again afterwards, it never reached the influent concentration and remained below 250 µg/L for the remainder of the experiment. The apparent continued contaminant destruction during the later stages of the experiment correlates with the continued presence of oxidant in the column, as indicated by the still elevated EC readings at the end of the experiment. This observation is similar to that made during Test 1.

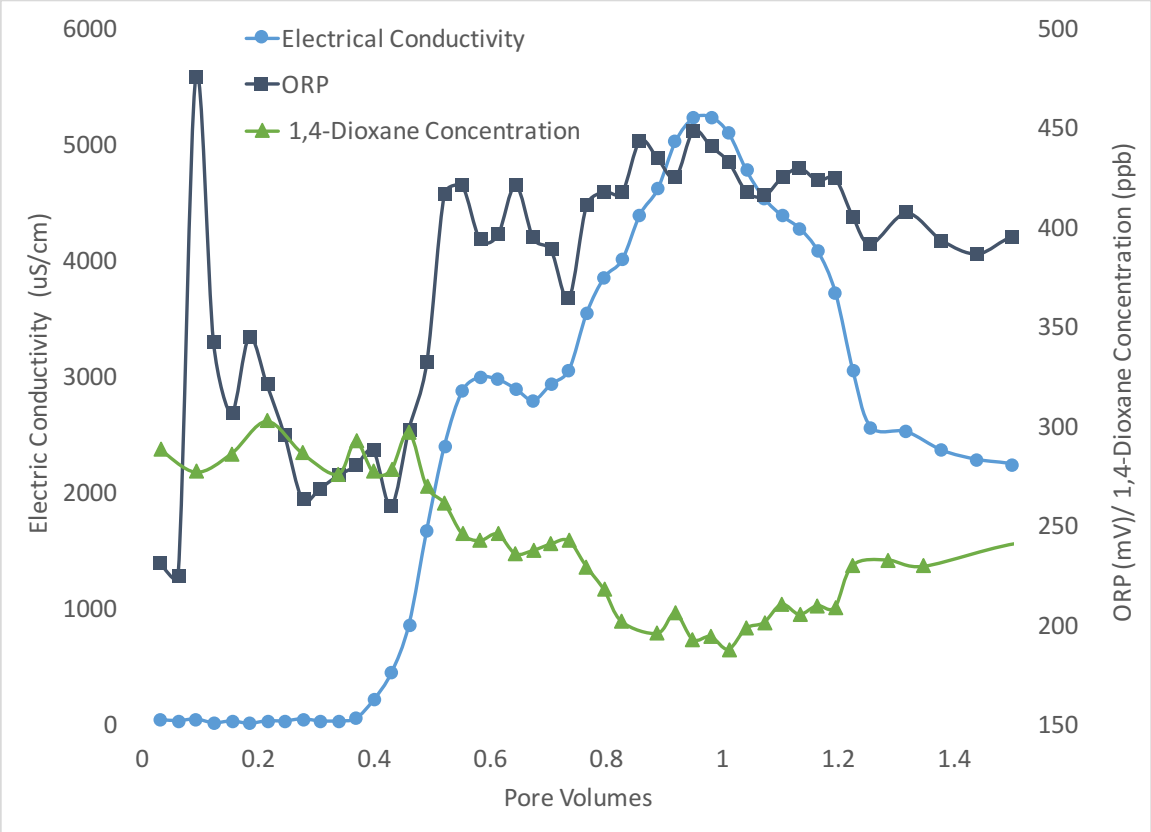

Figure 12: Results from Scenario I Test II: Electric conductivity and ORP readings with 1,4-Dioxane concentrations.

The 1,4-Dioxane degradation rates were calculated for the breakthrough of the first and second slug (Figure 13). The rates were similar with the breakthrough of the second slug having a rate that was slightly higher (0.2426 h^{-1}) than the first one (0.2001 h^{-1}).

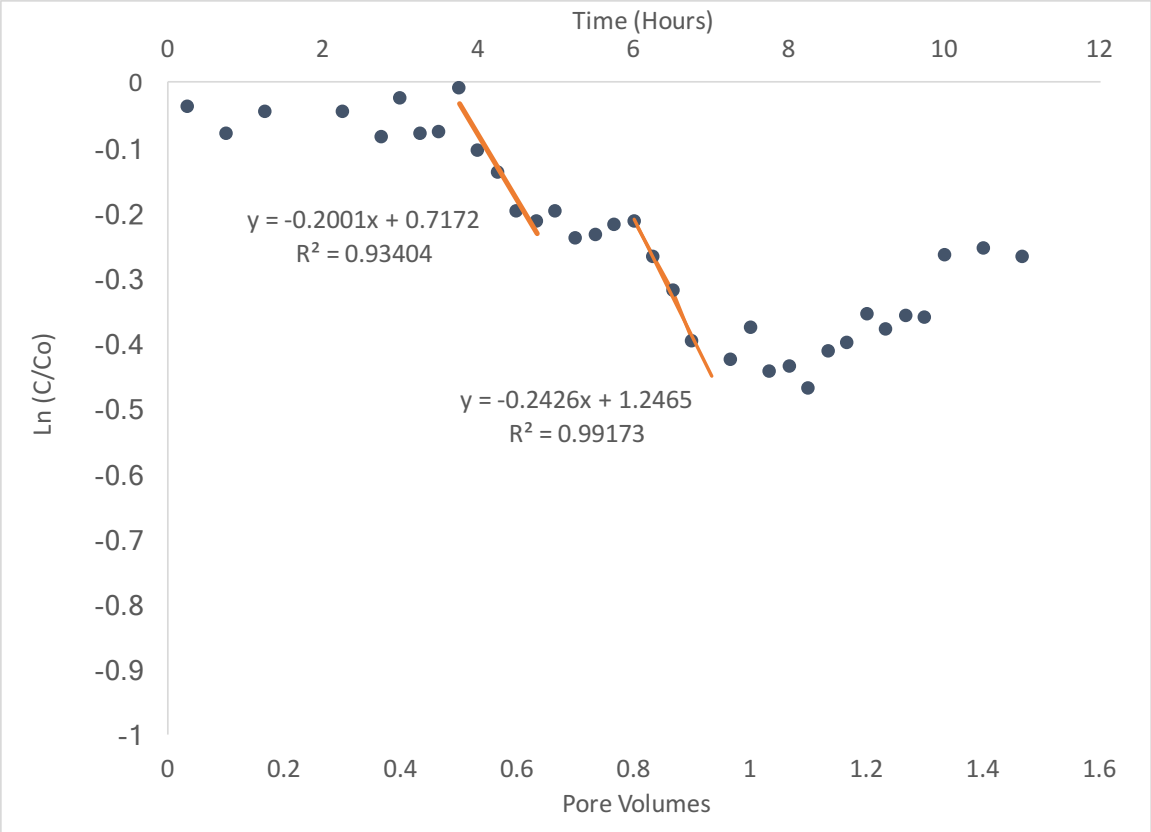

Figure 13: Results from Scenario I Test II: Pseudo first order reaction rates calculated from the breakthrough data of the first and second slugs.

TREATMENT SCENARIO II – *SINGLE SLUG INJECTION*:

The second treatment scenario simulated the injection of one slug of OxyZone directly into the base of the column. The duration of the experiment was 2.4 PV (approximately 20 hours). The same overall volume (200 mL) of oxidant solution was injected as in the Treatment Scenario I test. Figure 14 compares breakthrough curves for OxyZone and sodium chloride. Figure 15 compares the ORP and pH for Treatment Scenario II.

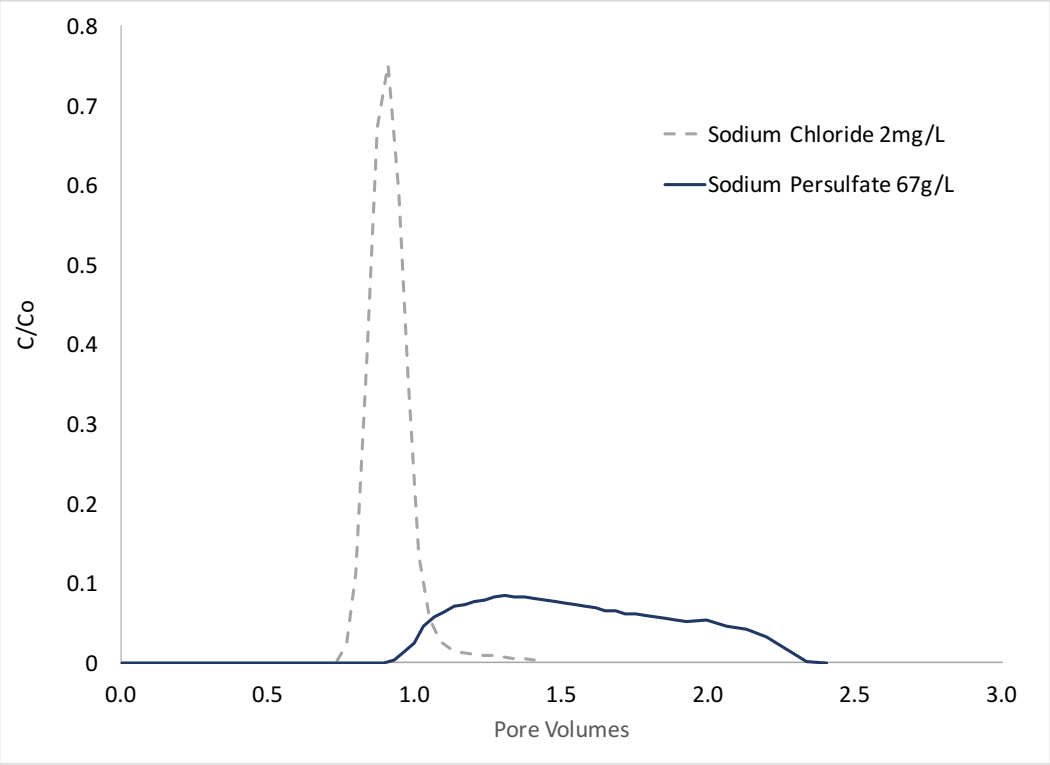

Figure 14: Treatment Scenario II – Single slug injection: Comparison between breakthrough curves for OxyZone and sodium chloride tracer.

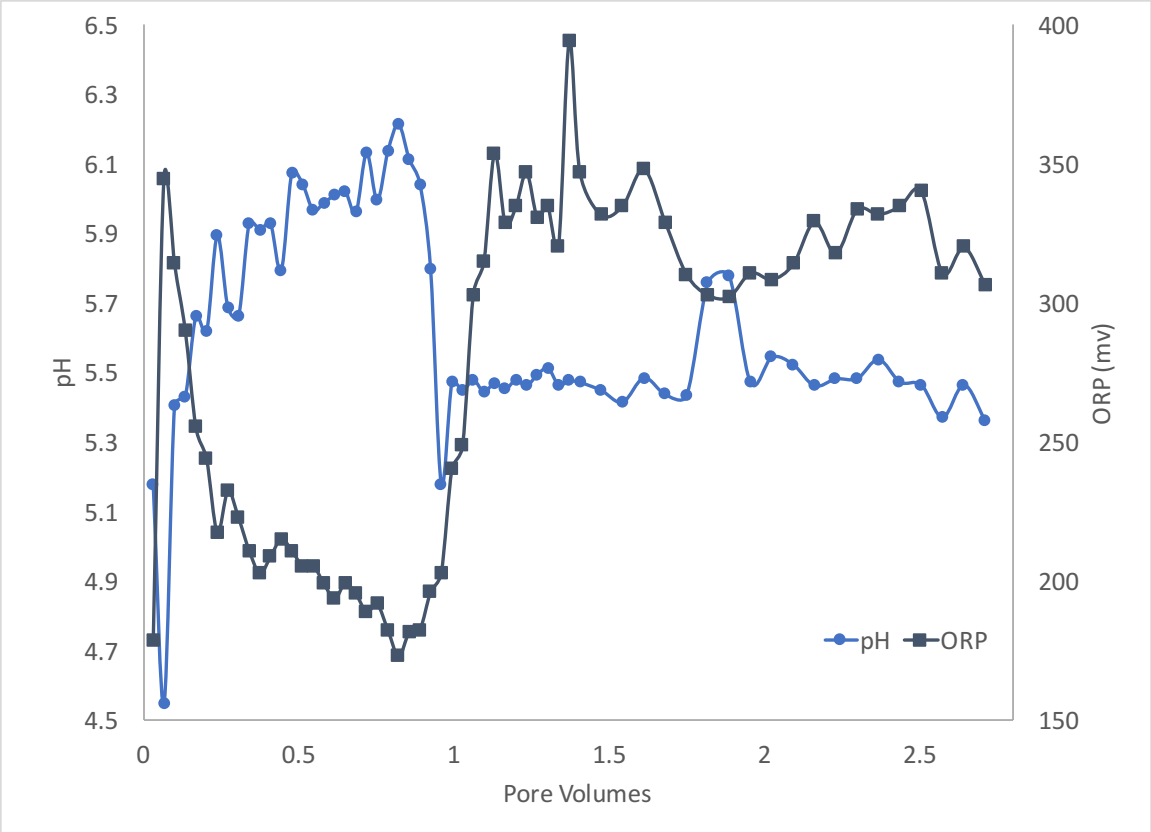

Figure 15: Results from Scenario II: ORP and pH of slug flow oxidation.

Figure 16 shows the 1,4-Dioxane concentrations, plotted for comparison against ORP, and EC data. The initial 1,4-Dioxane concentration was 287 µg/L. At 1 PV, the concentration dropped to <10 µg/L and fell below the limit of detection (3 µg/L) by 1.9 PV. The concentration of 1,4-Dioxane remained low until the end of the experiment (2.8 PV). This prolonged oxidation is mirrored in the ORP and EC data. This test was concluded when ORP and EC fell back to baseline levels, which was at the 3 PV mark. At that time, the 1,4-Dioxane concentration was still more than 80% than the corresponding column

influent concentration. Unlike Scenario I experiments, no sharp changes were observed in ORP and pH during the earliest stages of the experiment.

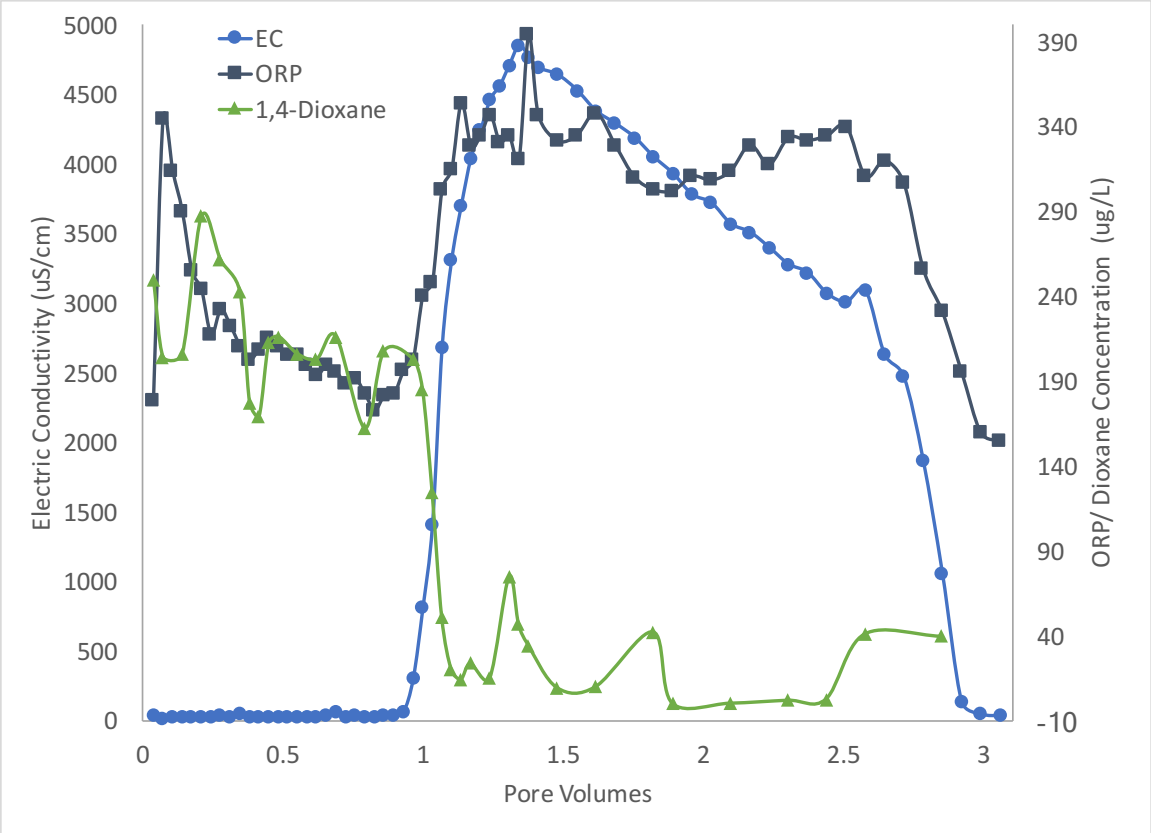

Figure 16: Results from scenario II: 1,4-Dioxane concentration. The EC and ORP data were included for comparison.

A linear trend line was fitted through leading edge of the 1,4-Dioxane breakthrough curve (Figure 17). The oxidation rate for this experiment was the highest of any of the experiments, with a rate constant of 1.5389 h^{-1}. The pseudo-first order reaction rate constants for all tests are summarized in Table 11.

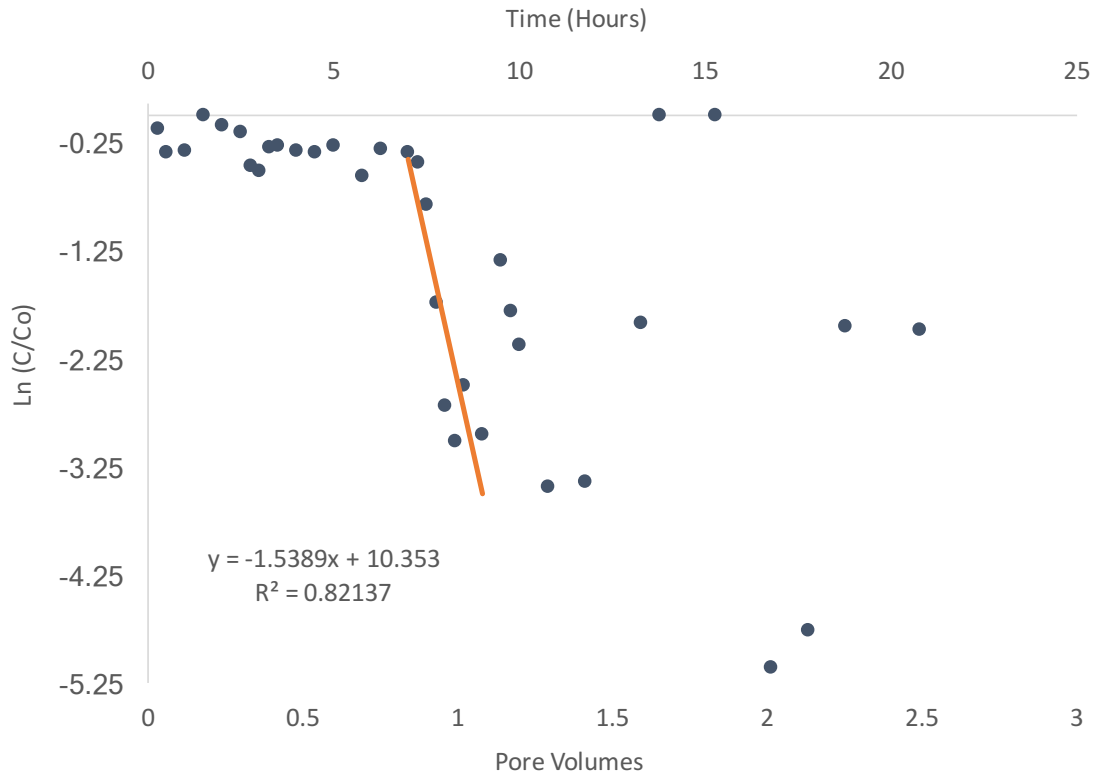

Figure 17: Results from Scenario II: Ln(C/Co) for pseudo-first order reaction rates.

	Scenario I – Test 1	Scenario I – Test 2a	Scenario I – Test 2b	Scenario II
k_1 (h^{-1})	0.08	0.20	0.24	1.54
$T_{1/2}$ (h)	8.57	5.97	6.99	0.45
R^2	0.85	0.83	0.83	0.82

Table 11: Reaction rates for all column experiments. Note that Test 2a and 2b refer to the reactions rates extrapolated from the first and second slug breakthrough (see Figure 13).

3.3 Results of EPR Experiments

EPR spectra are presented in Figures 19 to 21. The charts represent the first derivative of the absorption signals obtained by the EPR spectrometer. The magnetic field (x-axis) is in Gaussian units (10,000 Gauss is equal to 1 Tesla). The distance in magnetic force (Gauss) was measured between each spectrum peak to identify radicals. Figure 19 is the DMPO-OH spin trap spectrum, referred to as the blank. There are no distinct peaks in the blank that can be defined as radical species. Figure 20 shows an example of a hydroxyl radical spectrum. This specific spectrum is from a mix of DMPO, H_2O_2, and 1,4-Dioxane. The hydroxyl radical's signature is four peaks with a 1:2:2:1 intensity ratio. The hydroxyl radical spectra were identified using α_N=14.9 and α_H=14.9 (Mottley and Mason, 1988) and verified by WinEPR software. Figure 21 shows the DMPO/sodium persulfate spectrum and provides evidence for $\bullet SO_4$ radicals, with α_N=13.9G, and α_H=10.1 G (Harbor and Hair, 1972). The sulfate peaks appear obstructed by the hydroxyl radical, which is likely why the $\bullet SO_4$ radicals were not identified through WinEPR. The EPR spectra is identical in peak width to findings by Zhong (2015) that confirm presence of both hydroxyl and sulfate radicals. However, the references used in Zhong et al. (2015) to identify the sulfate radical are in fact for a sulfite addict. Therefore, this EPR cannot confirm the presence of the sulfate radical. It is noted that there was an increase in signal intensity for hydroxyl radical EPR spectra, suggesting increased hydroxyl radicals are produced in samples with sodium persulfate.

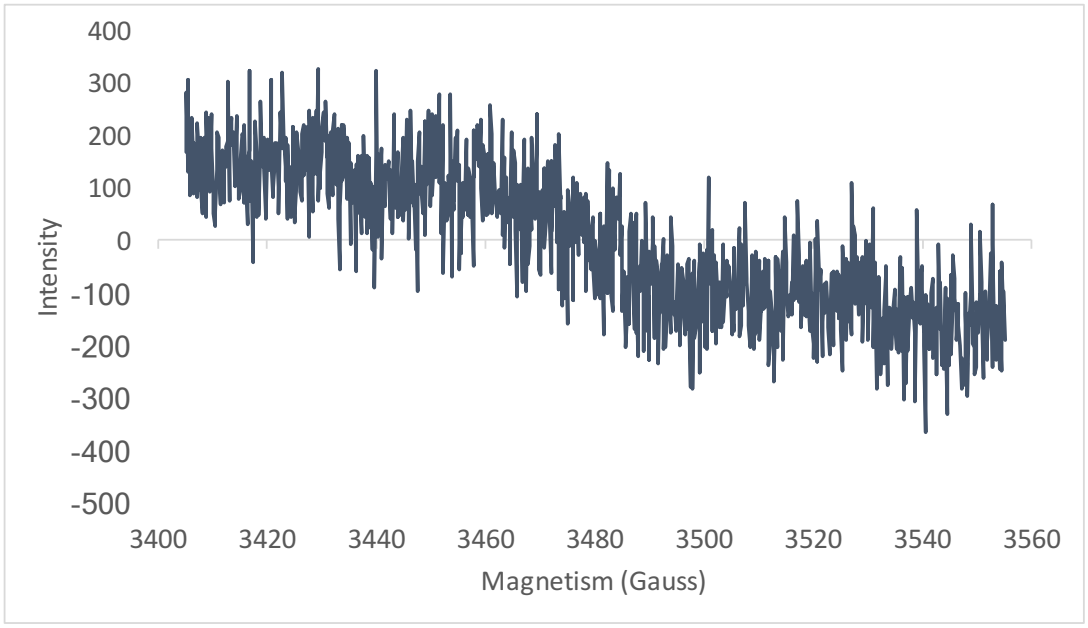

Figure 18: DMPO blank activated with UV light.

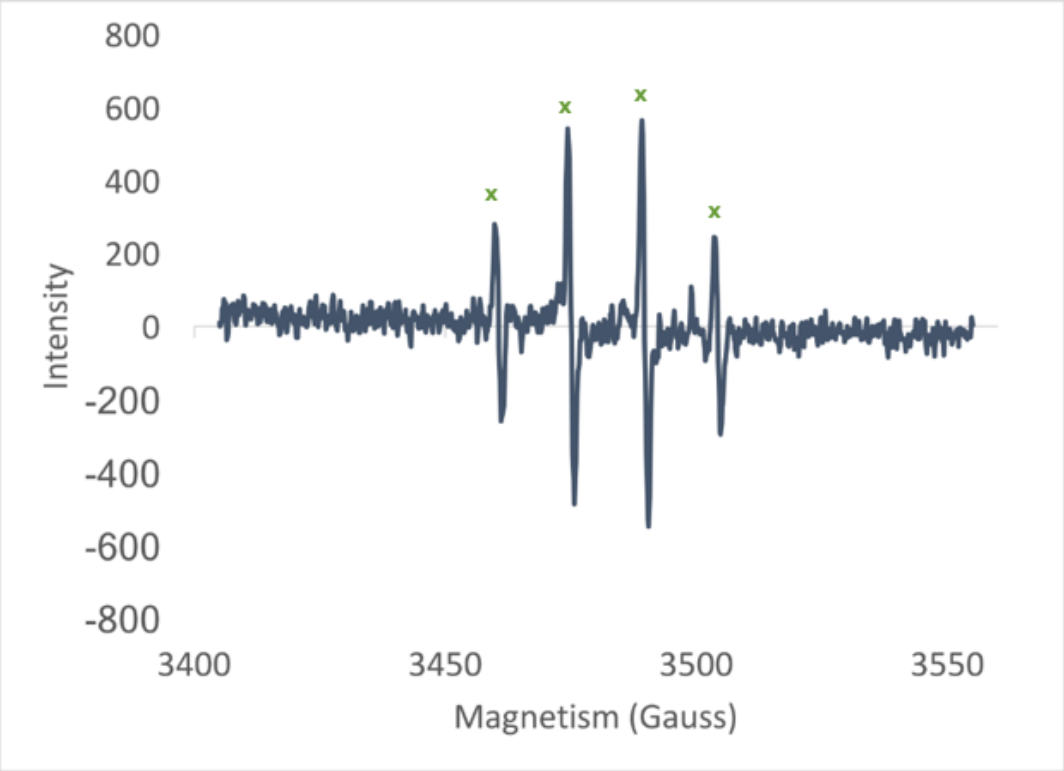

Figure 19: Hydroxyl radical produced by hydrogen peroxide, DMPO, and 1,4-Dioxane. The hydroxyl radical's signature is four peaks with a 1:2:2:1 intensity ratio.

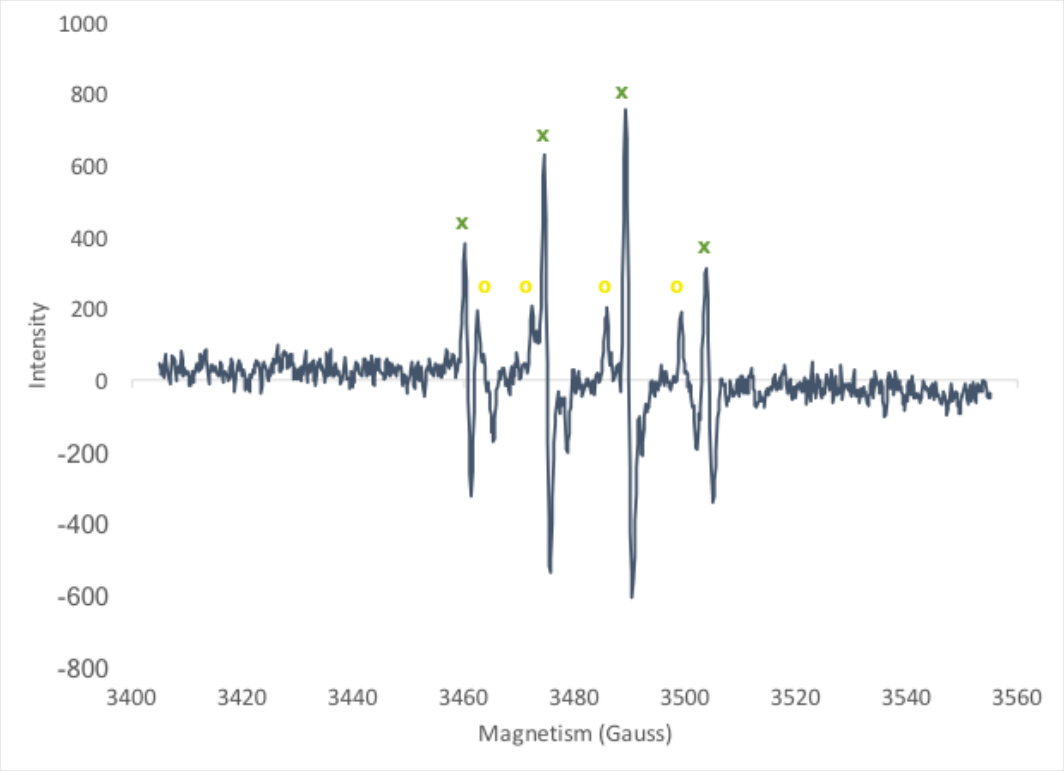

Figure 20: Hydroxyl and potential sulfate radical spectra from sodium persulfate and DMPO.

Figure 21 shows the EPR spectra obtained from OxyZone with UV light and DMPO. Similar to Figure 20, there is strong evidence that sulfate radicals exist in addition to the confirmed presence of hydroxyl radicals. The four peaks of the hydroxyl radicals are indicated with green “x” above each peak. The sulfate radicals are indicated by yellow “o”. When 1,4-Dioxane is added to the same mixture, the peaks disappear. This suggests that radicals are obstructed when interacting with 1,4-Dioxane, which supports the conclusion that OxyZone is interacting with the contaminant.

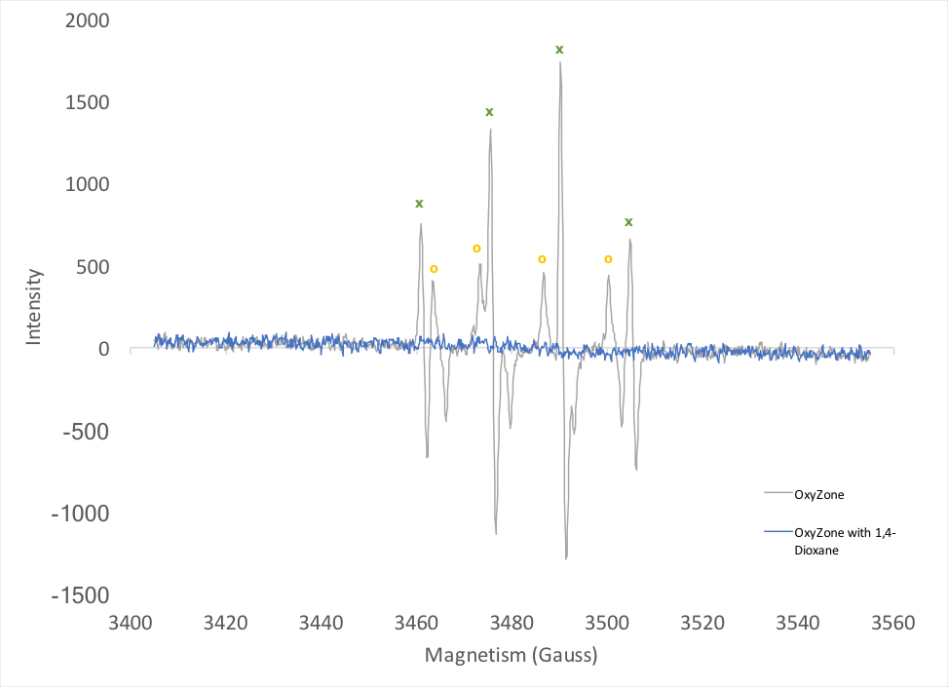

Figure 21: OxyZone EPR spectra with and without 1,4-Dioxane.

Several EPR samples were retained and stored at room temperature for a period of several days. These samples were re-run to determine if radicals were still being formed. Figure 22 shows an EPR spectra for sodium persulfate and hydrogen peroxide, after an incubation of 22 hours at 25 ˚C. Figure 23 shows EPR spectra for sodium persulfate activated with UV light after 5 days. Together these spectra provide evidence that radical production is still occurring after several days.

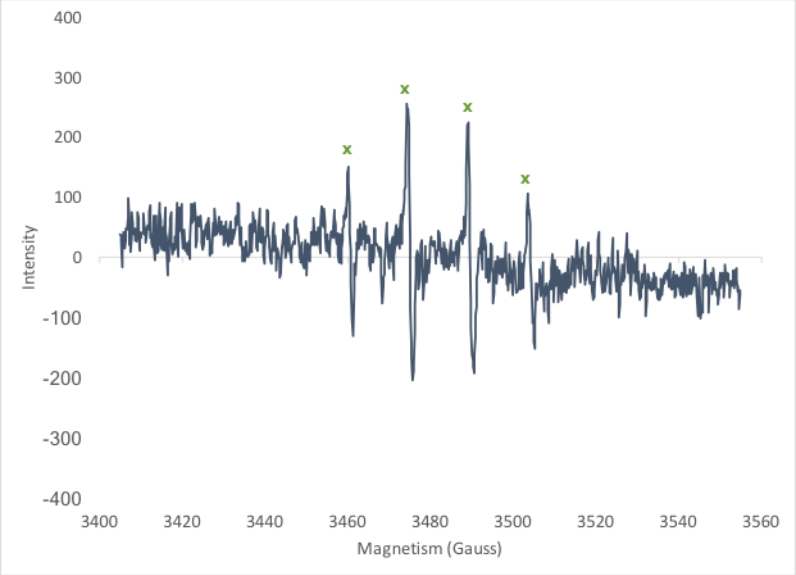

Figure 22: Sodium persulfate and hydrogen peroxide at 22 hours.

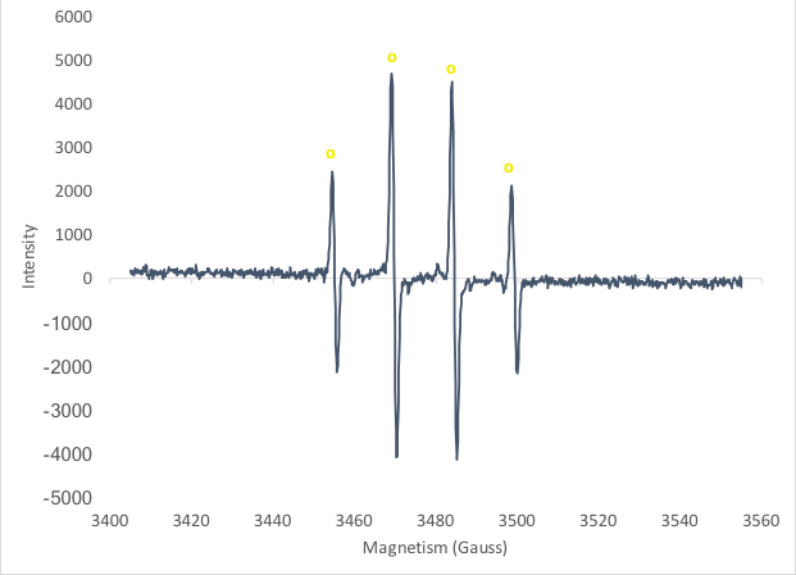

Figure 23: Sodium persulfate activated with UV light after 5 days in storage.

DISCUSSION

The principal objective of this study was to investigate the degradation of 1,4-Dioxane by an oxidant (OxyZone) under dynamic, flow through conditions that mimic the *in-situ* treatment of groundwater plumes. Initial batch experiments were conducted to determine 1,4-Dioxane degradation rates in the presence of porous material under static conditions. The reaction rates of 1,4-Dioxane oxidation with OxyZone in the presence of sediment were determined. This study's secondary objective was to identify the radicals produced during oxidation of 1,4-Dioxane water with OxyZone.

4.1 Batch Experiments

At an oxidant: contaminant ratio 250:1 and in the presence of porous material, the pseudo-first order rate constant was 0.0213 h^{-1} with a half-life of 33 hours. The observed rate was approximately 2.5 times lower than compared to Eberle (2016), who investigated rates in the absence of porous material. This finding implies that the degradation of 1,4-Dioxane by OxyZone proceeds more slowly when injected into a porous matrix relative to treating aqueous phase contamination, as one might be required when treating extracted groundwater *ex-situ*.

4.2 Column-Scale Experiments

At real-world contaminated sites, 1,4-Dioxane is predominantly present in a dissolved state, forming elongated plumes of contaminated water. Hence, its in-situ treatment would likely require the injection of a solution containing a reactive agent,

such as OzyZone. On this backdrop, two different oxidant injection schemes were tested (*Scenarios I and II*).

The column's basic flow properties were first investigated with a conservative tracer test. The normal distribution of the tracer breakthrough curve indicated that flow field is homogenous and not likely influenced by preferential pathways (Figures 7 and 15).

SCENARIO I EXPERIMENTS:

The greatest decline in 1,4-Dioxane concentration was observed during Scenario I – Test II, when column effluent concentration dropped to C/C_o=0.62 during the time when mixed with oxidant solution. Even after 1,4-Dioxane concentration rose again to about C/C_o=0.82, after most of the oxidant had already washed out of the column, it never reached the influent concentration for the remainder of the experiment. This suggests that the remaining oxidant fraction continued to destroy the dissolved contaminant past the time expected for a solute traveling at the speed of groundwater. The reason for the apparent retardation of the persulfate was not further investigated, but it is beneficial for the in-situ treatment and prolonged oxidation time.

The Scenario I column experiments also demonstrated that it is more advantageous to slowly inject the oxidant solution into the contaminated flow field. That is, quick injection concentrates the slug within a relatively small fraction of the porous space and therefore exposes the reactive agent to only a small fraction of dissolved

contaminant. Although the moment analysis suggests that the injectate is subject to retardation and tailing (Figure 15), i.e. the oxidant is traveling slower than the plume, the absolute difference in travel time in this column system is not large enough to cause major mixing with 1,4-Dioxane present in pores not filled with the oxidant. This was indicated by similar arrival times of the EC peaks relative to that of a conservative solute (Figure 15). Hence, contaminant destruction is confined to a limited fraction of the pore space. However, when injected slowly, the oxidant solution is mixed into a larger fraction of pore space, resulting in more contaminant destruction. This is expressed in the prolong period of much lower 1,4-Dioxane concentration in the column effluent during Scenario I – Test II relative to Test 1.

The Scenario I test also demonstrated that the pH decline correlates with a rise in ORP (Figure 9 and 11). This result was expected because as the oxidant advances (indicated by the rising ORP), sulfate (SO_4^{2-}) is produced. Sulfate is a weak conjugate base, which leads to the production of sulfuric acid (Kolthoff and Miller, 1951). The formation of sulfuric acid is partially encountered by the phosphate buffer, which is part of the OxyZone formulation. However, sufficient acid is produced to lower the pH to less than 6.5. In general, the pH value during persulfate treatment is a function of the solution's buffering capacity and the oxidant dosage (SERDP, 2011).

Unlike EC readings, which have been found additive when two slugs overlap (Figures 8 and 12), ORP readings were not much higher during the same period. In terms of increasing the strength of the oxidant solution, this result indicates that there is no

immediate benefit by overlapping slugs of similar strength. However, it should be possible to increase the ORP by injecting fresh oxidant solution into the porous medium where oxidant strength has dropped by either consumption or dilution.

Similar to prior research by Eberle (2016), the degradation of 1,4-Dioxane was modeled with pseudo-first order kinetics. The rate of degradation for Scenario I ranged from 0.088 h^{-1} to 0.116 h^{-1} at an oxidant: contaminant ratio of 250:1 (Table 11). For a system without porous media but at the same oxidant: contaminant ratio, Eberle et al. (2016) predicted a rate of k=0.2906 h^{-1}, which is 2.5 times greater than found in this study. This result underlines the importance of accounting for the porous material and its properties when planning for an injection of oxidant into a polluted aquifer.

SCENARIO II EXPERIMENTS:

In terms of degrading 1,4-Dioxane, the injection of one slug at the base of the column was the most successful treatment scenario, resulting in complete destruction of the contaminant over a prolonged period of time (Figure 17). The rate of destruction was more than an order of magnitude faster than any other experiment (Table 11). In fact, the projected rate for 1,4-Dioxane degradation with OxyZone at 7,400:1 oxidant: contaminant ratio would be k=7.44 h^{-1} (Eberle et al., 2016). The projected rate reaction calculated in this study with the same oxidant: contaminant ratio is k=1.539 h^{-1}, which is 4.83 times slower than reported by Eberle et al. (2016). On the background of the mixing

argument made when discussing the effectiveness of fast versus slow injection (Scenario I - Tests 1 and 2), it seems counterintuitive that the injection of one slug should result in better contact with the contaminant in solution; however, the Scenario II experiment was different in two regards. First, the slug was injected farthest away from the effluent and therefore traveled longer through the column than under Scenario I. This prolonged residence time in the column magnified the dispersion of the slug, as indicated by the long spread of the breakthrough curve in relation to the conservative tracer (Figure 15). Dispersion and mixing provided better contact of the oxidant with 1,4-Dioxane, hence greater treatment. Second, the slug was injected more slowly, relative to Scenario I at the rate of 4 mL/minute. The slow injection distributed the slug over a larger fraction of the column pore volume. Together, this injection scheme resulted in prolong and faster treatment, as measured by the pseudo first order reaction rate.

Also, unlike Scenario I experiments, no sharp changes were observed in ORP and pH during the earliest stages of the experiment. This finding suggests that the anomalies during Scenario I are most likely caused by the act of injecting oxidant solution directly into the column, rather than column inlet. Although not further investigated, it must be assumed that the hydraulic pressure from quickly injecting oxidant solution into a saturated confined column momentarily disturbed the flow system and possibly pushed a small, but noticeable amount of oxidant solution deeper into the column. This would explain why the observed anomaly occurs well before the expected breakthrough of the bulk oxidant.

Although identical volumes were used in both tests (0.1 PV each), the conservative tracer resulted in a sharp peak, while the OxyZone breakthrough was drawn out. This is partially due to the time it took for injecting the NaCl slug (33 min) versus 45 min for the OxyZone. The recovered mass of OxyZone (M^0) was 76.67% while the center of mass (M^1) was located at 1.5 PV. Also, the OxyZone displayed a right-skewed distribution, which suggest significant tailing of solute.

A hypothesis was tested to determine if the density of OxyZone was responsible for the drawn-out breakthrough curves seen during column scale tests. A second sodium chloride tracer test was conducted, but with a concentration of 67 g/L NaCl and a density of approximately 1.05 g/cm^3 (Appendix Figure C4). This density was chosen to mimic the density of OxyZone. The data showed that the movement of OxyZone through porous media is partially density driven, i.e. the shape of the breakthrough curve was similar to the Oxyzone one and distinctively different from the low concentration NaCl tracer testy (C_{NaCL} = 2 g/L; Density = 1.0) (Fig. 7). The density driven advection slowed down the movement of the OxyZone in the column system and prolong the contact time with the 1,4-Dioxane contaminant, increasing its destruction.

4.3 EPR

The data in Figures 19-21 as well as Appendix C4-C23 confirmed that radical formation was occurring during the oxidation of 1,4-Dioxane with OxyZone. The hydroxyl radical was observed in virtually all EPR runs that included ozone, sodium persulfate, or activated hydrogen peroxide. There was evidence for the presence of the sulfate radical

but its EPR signal appears to be dwarfed by the omnipresent hydroxyl radical. The presuming sulfate radical peaks resembled the sulfate radical spectrum reported by Zhong et al. (2015). The spectra that Zhong (2015) achieved for identification of sulfate radicals is identical to what was obtained in this study (Figures 19-24); however, these spectra could not successfully be identified as sulfate radicals using WinEPR.

One of the difficulties of accurately identifying radicals from prior studies was questionable literature data. For instance, Zhong (2015) describes the presence of sulfate radicals when activating persulfate with iron. This proved to be problematic for several reasons. The first being that Zhong et al. (2015) methodology was based on Yan et al. (2015), with particular reference to their values for hyperfine coupling parameters. However, the parameters used in both of these studies are actually for a sulfite adduct, and not a sulfate radical. These parameters skew the EPR spectra when analyzed with WinEPR and ultimately weaken the integrity of the published data.

In addition, the EPR spectra that Zhong et al. (2016) obtained were also problematic. When examining their DMPO-OH blank, there are three peaks in the spectra that indicate contamination of the blank. The same spectrum is obtained when combining DMPO with iron shavings. This impurity challenges whether or not the iron was actually responsible for activating the sodium persulfate to produce the sulfate radicals in solution.

Continued hydroxyl radical formation was proven through EPR spectrometry for many samples (Figures 20-24). This data suggest that radical formation takes place during the oxidation of 1,4-Dioxane in the presence of OxyZone. However, many of the EPR spectra with hydroxyl radical signatures were activated with UV light. OxyZone is branded as a peroxone activated persulfate. The absence of radicals without activation from UV light questions whether or not the persulfate is actually activated by the addition of H_2O_2. The EPR spectra for OxyZone shows confirmed hydroxyl radicals and suggested sulfate radicals. This spectrum disappears when 1,4-Dioxane is introduced to the solution, indicating that the oxidation of contaminant obstructs radical formation.

There were several shortcomings to parts of the study that must be considered when discussing the EPR readings. The EPR spectrometer was a fairly dated instrument and it was located in another building relative to where the OxyZone generator was located. Because the oxidant mixture is unstable, particularly its ozone compound, samples had to be deep-frozen in liquid nitrogen to retard the reactions happening inside of the EPR samples. The delay in transporting the sample to the EPR instrument together with temperature fluctuations while walking the samples across campus, may have had an impact on the data quality.

CONCLUSION

Peroxone activated persulfate oxidation of 1,4-Dioxane was achieved in both batch and column scale experiments using OxyZone as the oxidizing agent. In batch scale

experiments, 1,4-Dioxane was degraded at the rate of 0.0213 h^{-1} at the molar oxidant: contaminant ratio of 250:1. In the three column experiments, the degradation rates varied from 0.0808-1.5389 h^{-1}. The EPR data confirmed the formation of hydroxyl radicals in OxyZone, and suggests the formation of sulfate radicals. This data is supported by the prolonged contaminant oxidation that takes place in both batch and column scale experiments. This research supports the development of ISCO of 1,4-Dioxane in groundwater plumes. ISCO is a valuable technology for its cost and energy effective capabilities to remediate contaminants. OxyZone's persistence in the system enhances ISCO capabilities by minimizing the volume of oxidant needed for remediation. This development allows for groundwater plumes to be remediated more quickly and cost-effectively relative to other, more short-lived oxidants.

The fact that spectra could not be confirmed with certainty requires further inquiry as to what the EPR spectra truly represents. Nevertheless, the high oxidation rates of the column-scale experiments coupled with the drastic changes in ORP and pH still suggests that sulfate radical formation is likely.

APPENDIX A: LIST OF ABBREVIATIONS

1,1,1-TCA	1,1,1-trichloroethane
AOP	Advanced oxidation process
ATSDR	Agency for Toxic Substances and Disease Registry
EC	Electric Conductivity
EPA	US Environmental Protection Agency
ISCO	In-situ chemical oxidation
ITRC	Interstate Technology and Regulatory Council
ORP	Oxidation Reduction Potential
PAP	Peroxone activated persulfate
PFAAs	Perfuluoroalkyl acids
PPB	Parts Per Billion
SERDP	Strategic Environmental Research and Development Program
SIM	Select Ion Monitoring
TCE	Trichloroethene
UCMR	Unregulated Contaminant Monitoring Rule
USAF	US Air Force

Table A1: List of abbreviations.

Sodium Chloride Concentration (mg/L)	2000	1000	500	200	20	2	0
Electric Conductivity (µS/cm)	3510	1904	959	414	40.09	3.46	1.06

Table B1: Sodium chloride calibration curve.

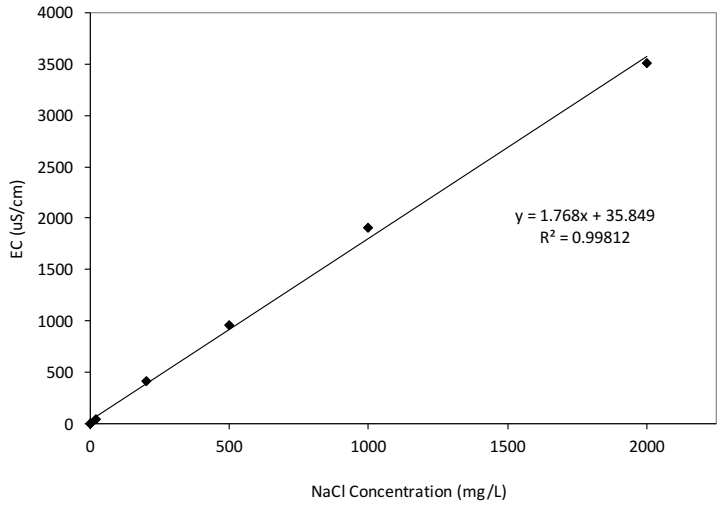

Figure B1: Linear relationship between electric conductivity and concentration of sodium chloride in solution.

Settings	Time (min) / Temp °C
Trap	
Trap Type	#7 Tennax
Sparge Mount	40 C
Sample	35 C
Purge Times & Temperature Parameters	
Purge Time	11 min
Dry Purge Time	1 min
Trap Temp	40 C
Water Management Temperature Parameters	
Purge Temp °C	120
Desorb Temp °C	40
Bake Temp °C	240
Bake Parameters	
Bake Time	10 min
Trap Temp °C	210
Desorb Time & Temperature Parameters	
Desorb Time min	0.5
Trap Temperature °C	190
Desorb Preheat °C	125
Trap Temperature Parameters	
Heated Zones	
Transfer Line °C	120

Valve Oven °C	120

Table B2: Purge and trap method settings.

Injector Temperature °C	240
Interface Temperature °C	230 C
Oven Temperature °C	45 (hold 4.5 min) to 100 (at rate of 12 C/min) to 240 (hold 1.3 min; at rate of 25 C/ min)
Column Inlet Pressure kPa	31.3
Column Flow	0.8 mL/min
Linear Velocity	31.5 cm/sec
Split ratio	35
Total Flow	28 mL/min
Detector	SIM mode m/z (88,58, 96, 64, 46)

Table B3: GC-MS method settings.

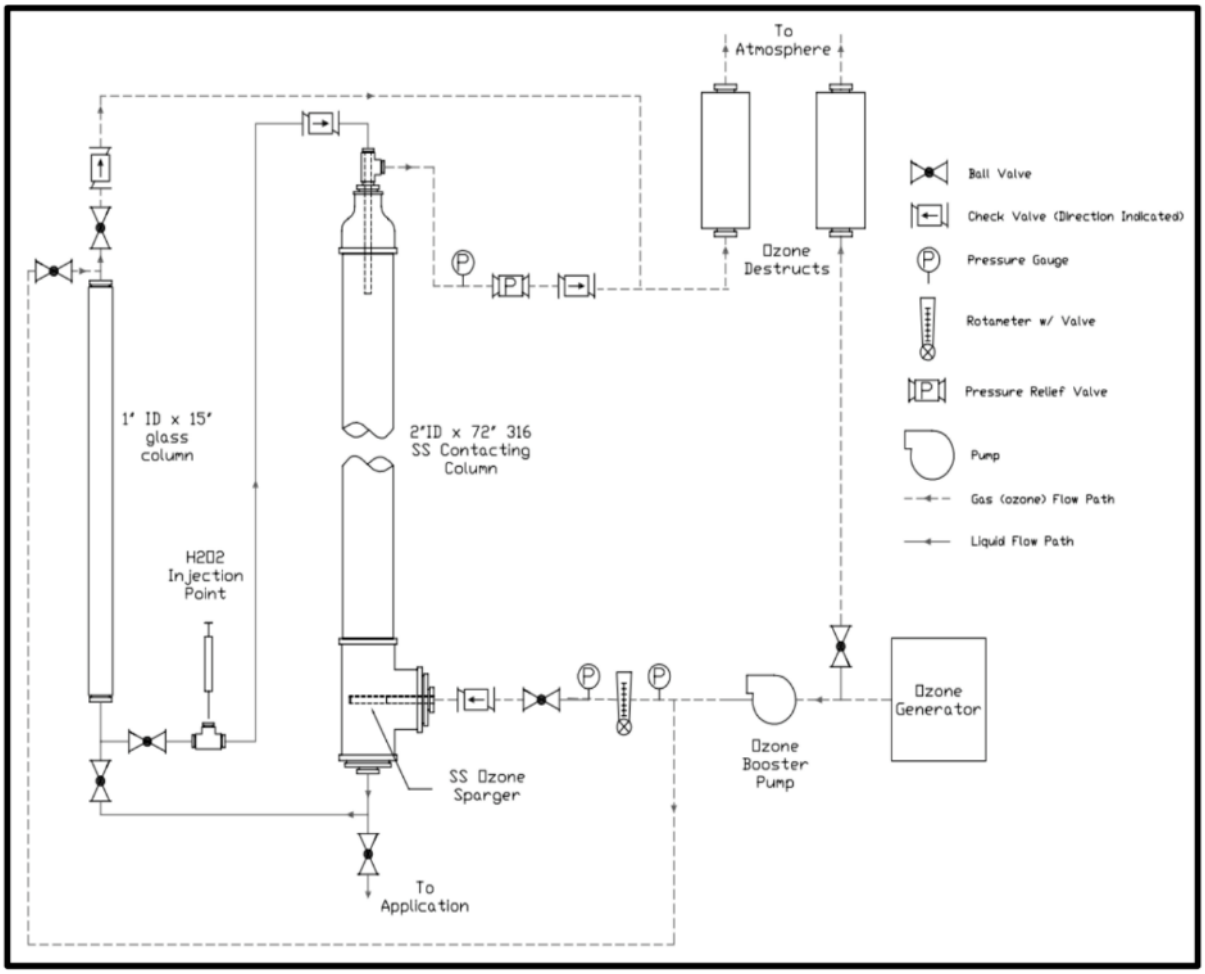

Figure B2: Diagram of bench-scale ozone generator.

	Control	100:1	250:1	500:1	1000:1
k_1 h^{-1}	0	0.0025	0.009	0.0348	0.0946
$T_{1/2}$ (h)	n/a	277	77	20	7

Table C1: Oxidation of 1,4-Dioxane over 24 hours at varying oxidant: contaminant molar ratios (0:1 [Control], 100:1, 250:1, 500:1, 1000:1).

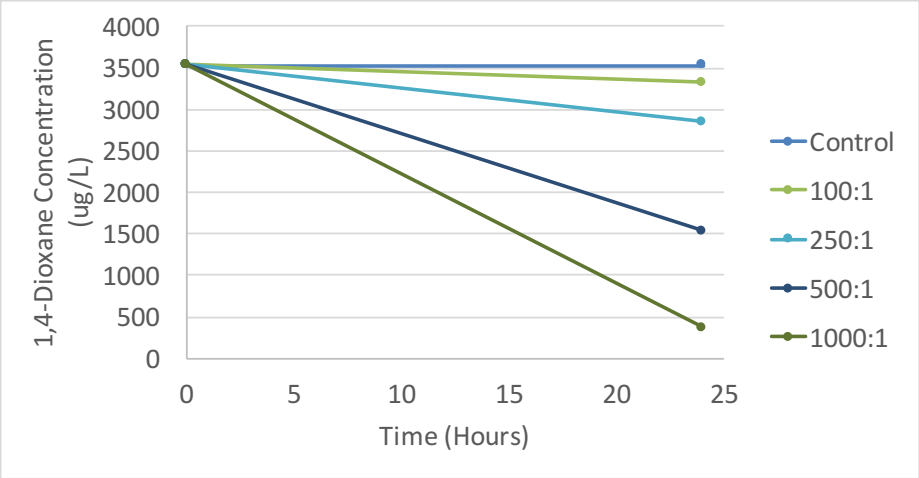

Figure C1: Concentration of 1,4-Dioxane in initial 24-hour pilot study.

	Control		250:1	
	pH	ORP (mv)	pH	ORP (mv)
T=0 hour	202.9	8,853	226.6	8.448
T=2 hours	183.1	8.301	187.6	8.187
T= 8 hours	212.2	8.241	167.5	8.171
T=1 day	243.9	6.535	226	8.201
T=2 days	165.5	8.055	183.7	6.717
T=4 days	143.5	7.469	166.9	7.793
T= 8 days	155.6	8.652	150.8	7.714
T= 16 days	137.2	7.996	166.9	6.865

Table C2: pH and ORP for 250:1 16-day batch scale pilot study.

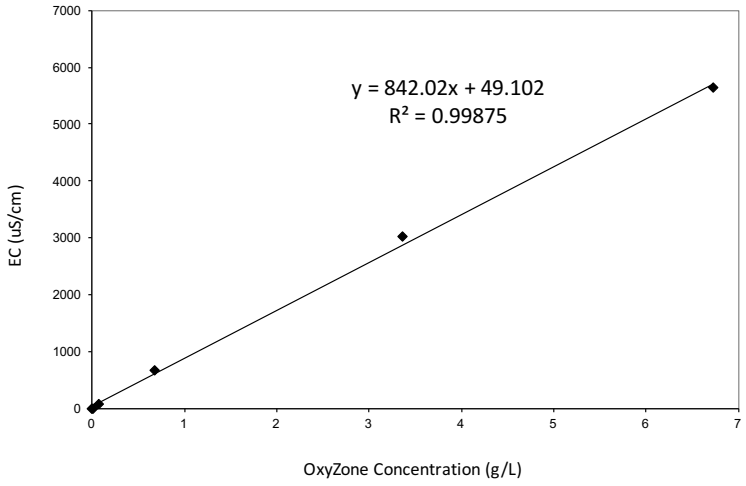

Figure C3: OxyZone electric conductivity calibration curve.

	M_O (%)	M_1 (PV)	M_2 (D_L)	M_3 (PV)
Scenario I, Test I	50.81	0.76	143	130
Scenario I, Test II	76.25	1.10	178	58
Scenario II	76.67	1.5	135	102

Table C3: Moment analysis data.

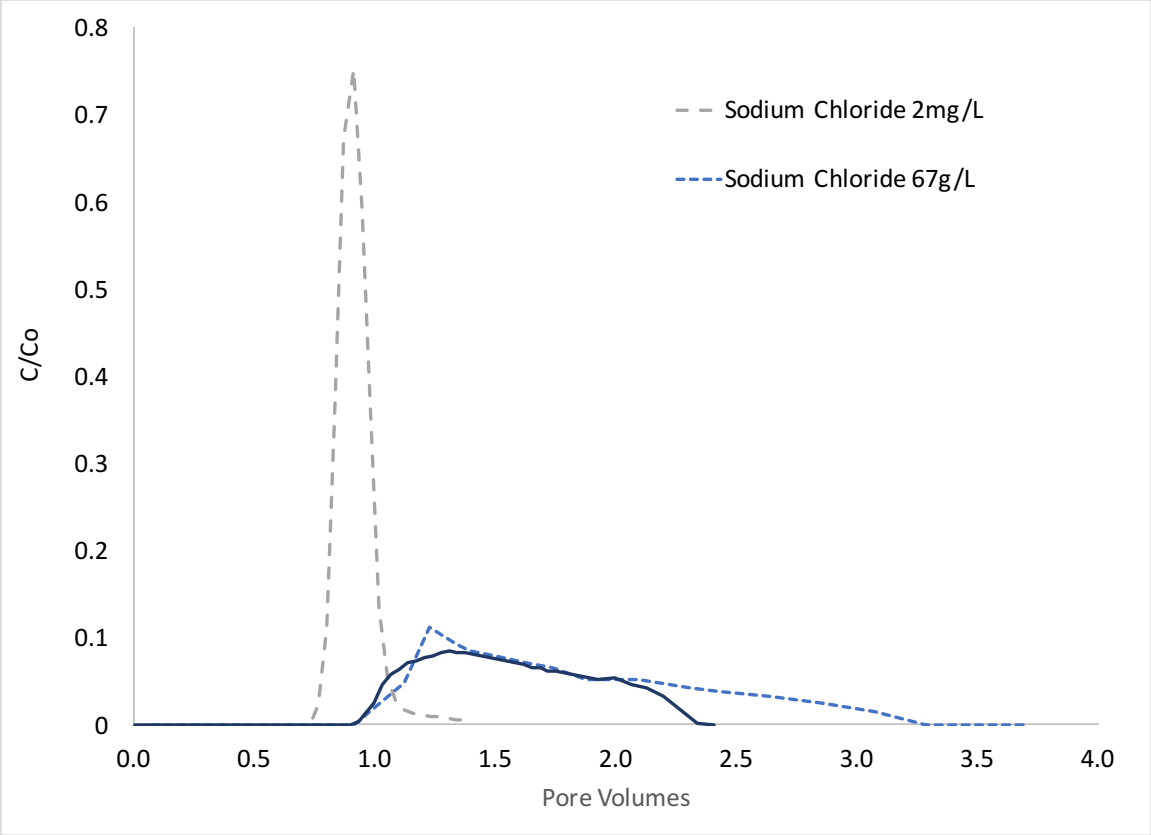

Figure C4: Sodium Chloride breakthrough curves as a function of concentration and density. The density of the dilute solution was approximately the same as water. That of the concentrated tracer solution was 1.05 g/cm^3.

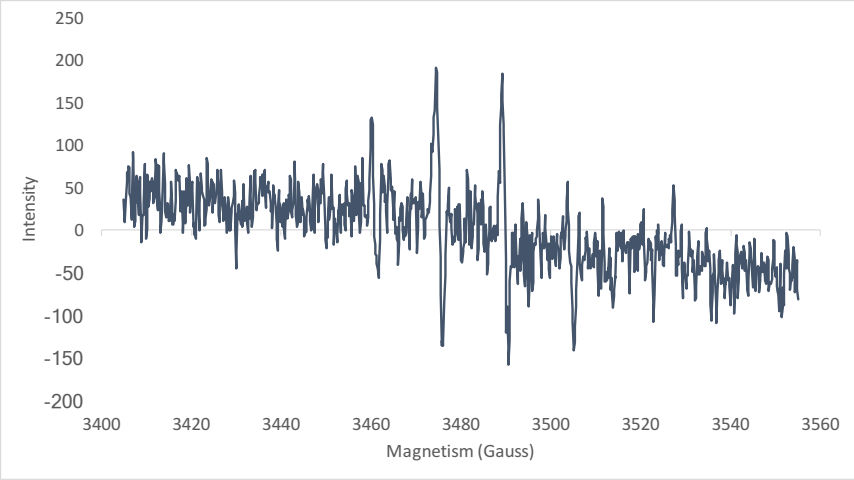

Figure C5: Sodium persulfate + 1,4-Dioxane.

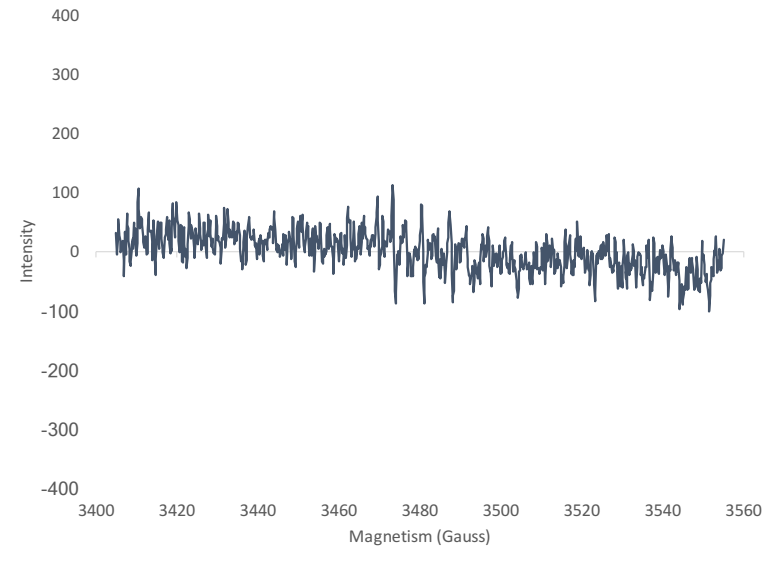

Figure C6: Disodium phosphate + ozone.

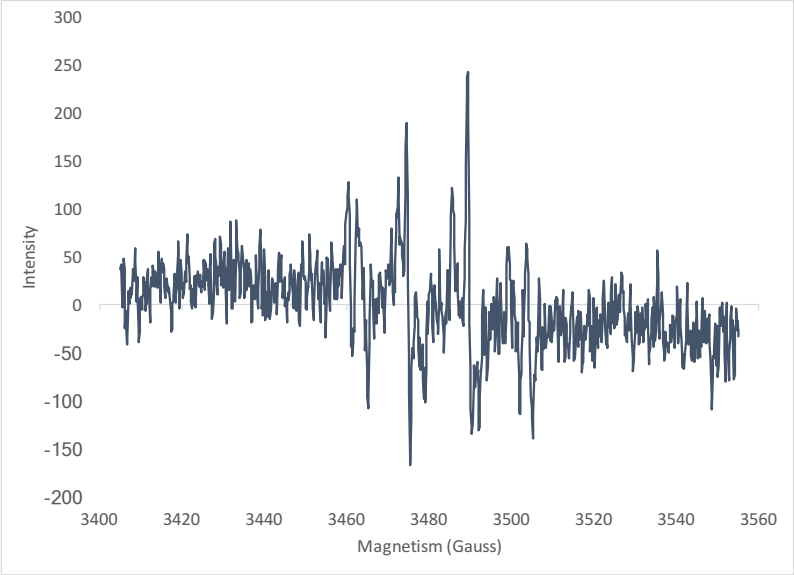

Figure C7: Sodium persulfate + UV light activated (3 min).

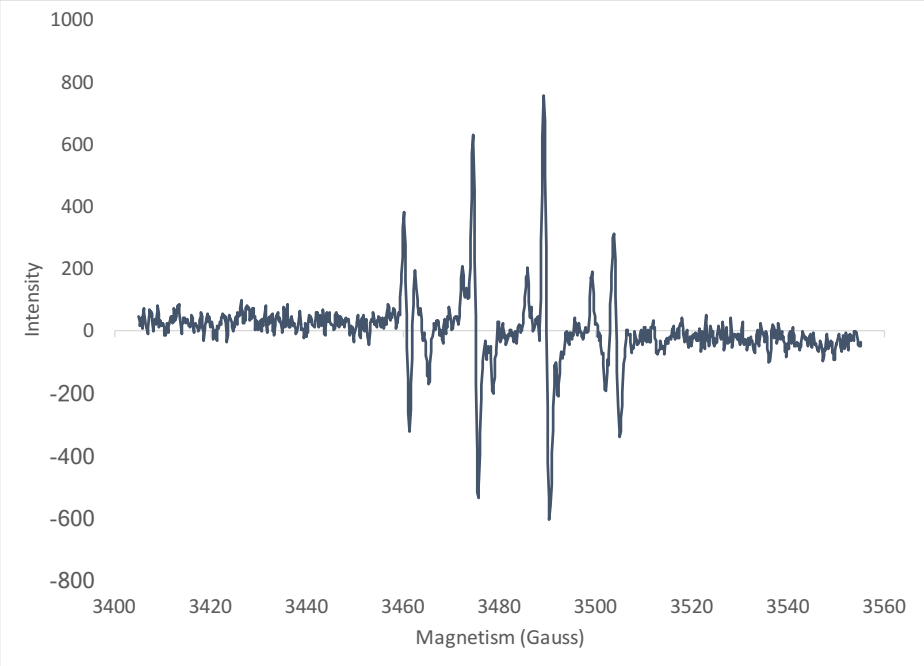

Figure C8: Sodium persulfate + UV activated light (4 min).

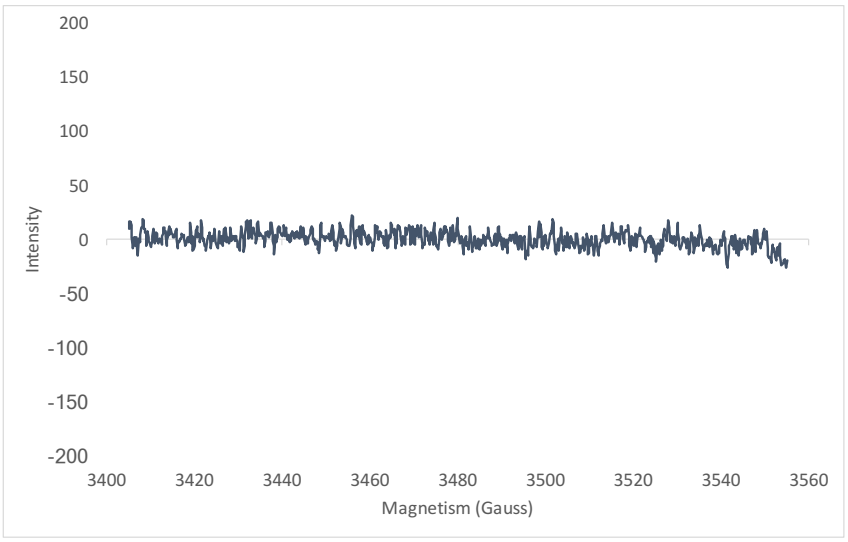

Figure C9: 1,4-Dioxane.

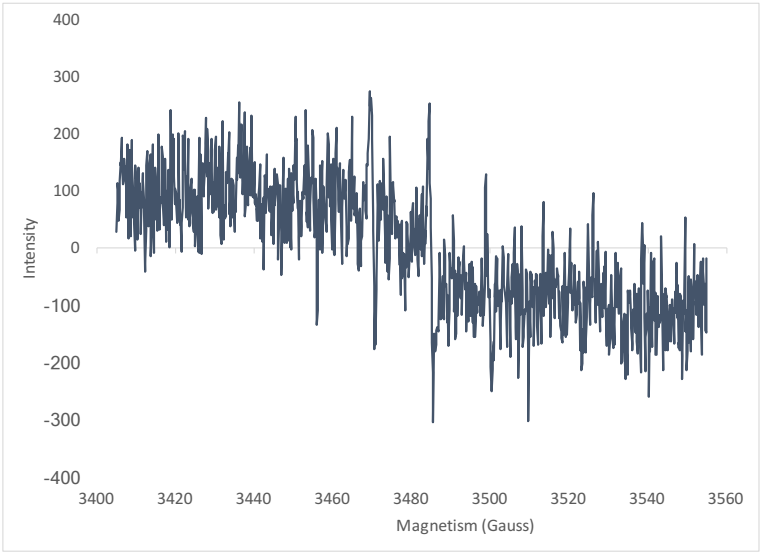

Figure C10: Hydrogen peroxide.

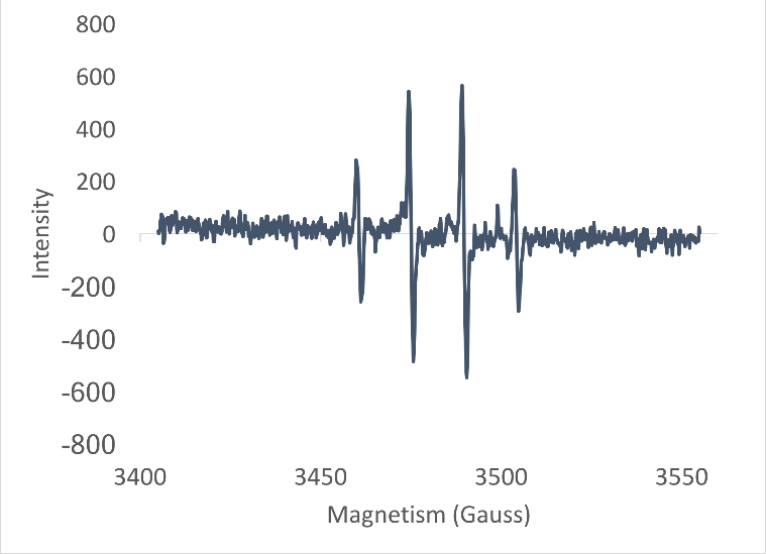

Figure C11: Hydrogen Peroxide activated with UV light.

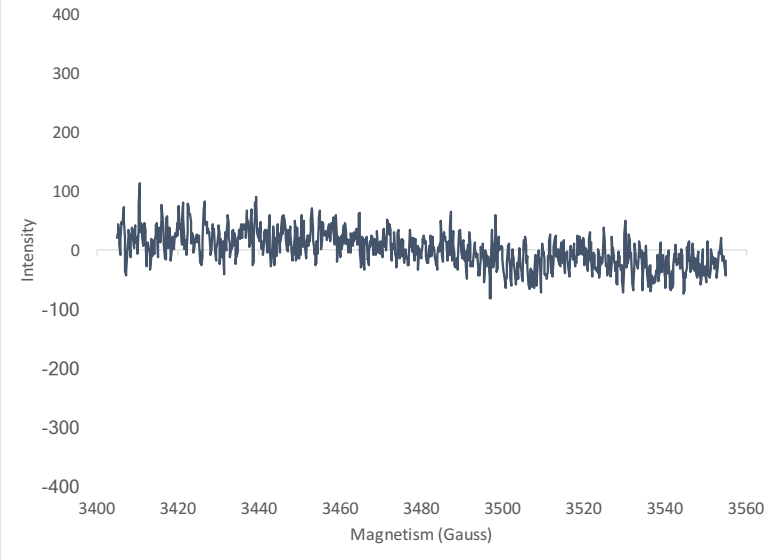

Figure C12: Hydrogen peroxide + 1,4-Dioxane.

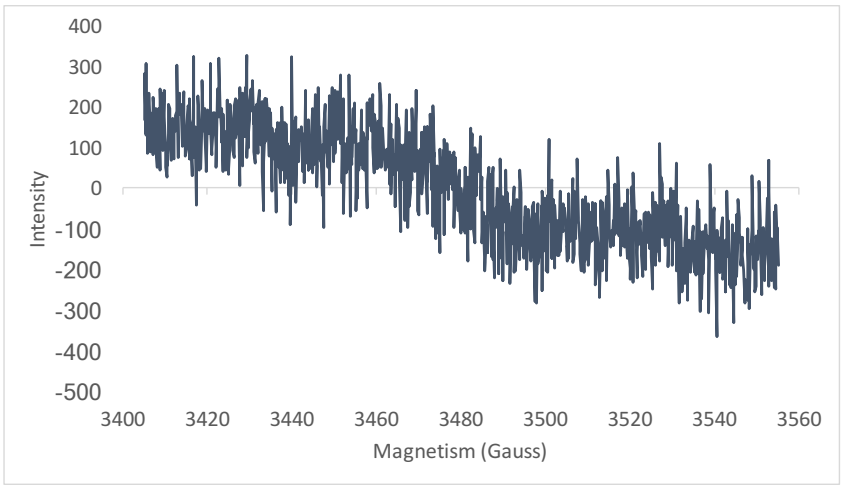

Figure C13: DMPO activated by UV light.

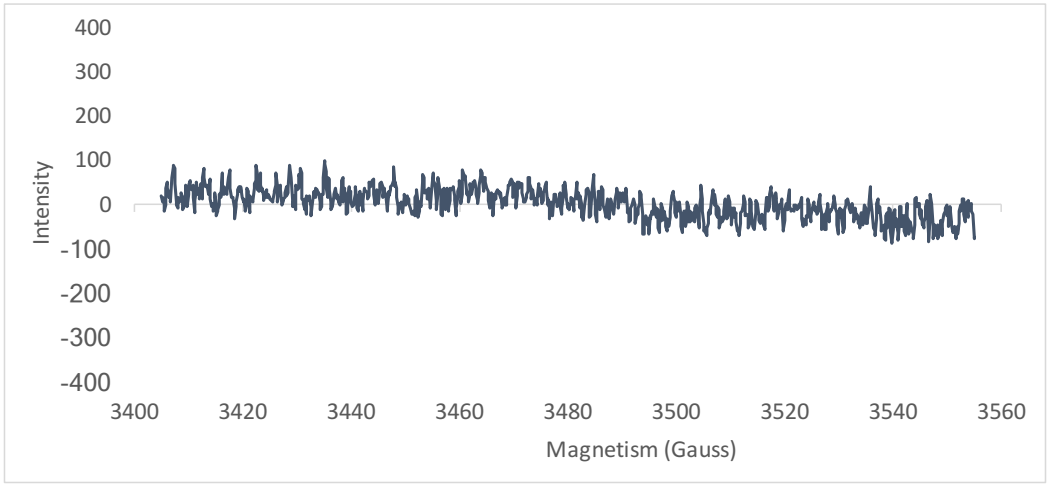

Figure C14: Sodium persulfate activated with UV light.

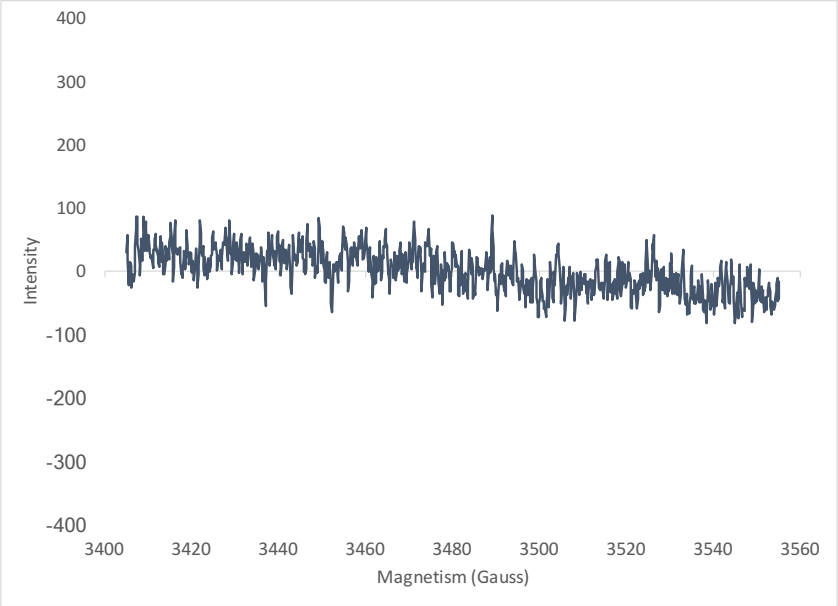

Figure C15: Sodium persulfate.

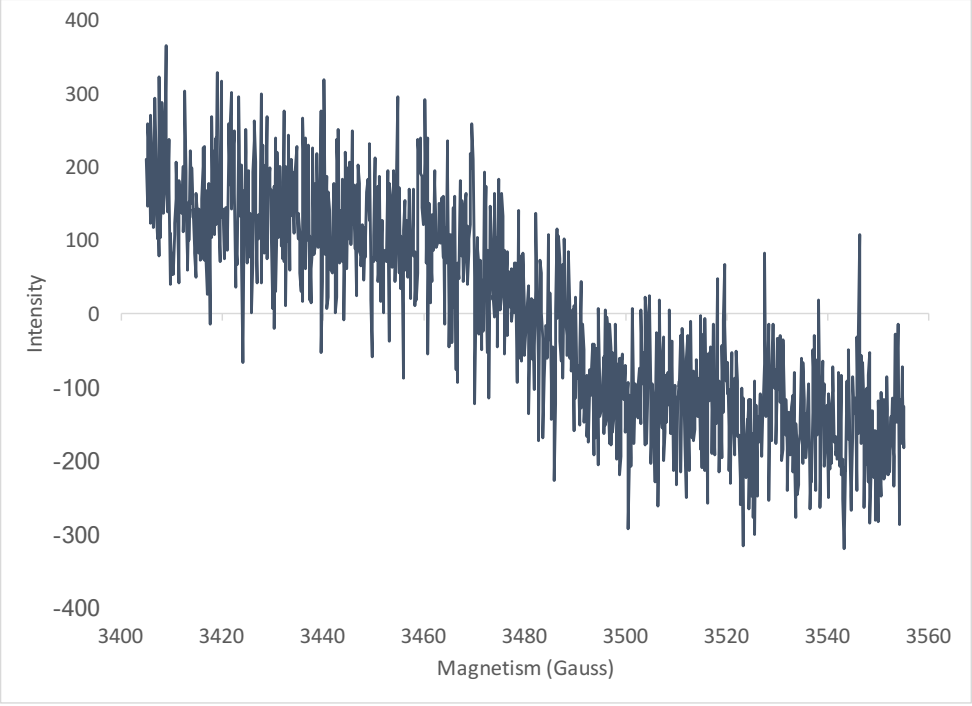

Figure C16: DMPO.

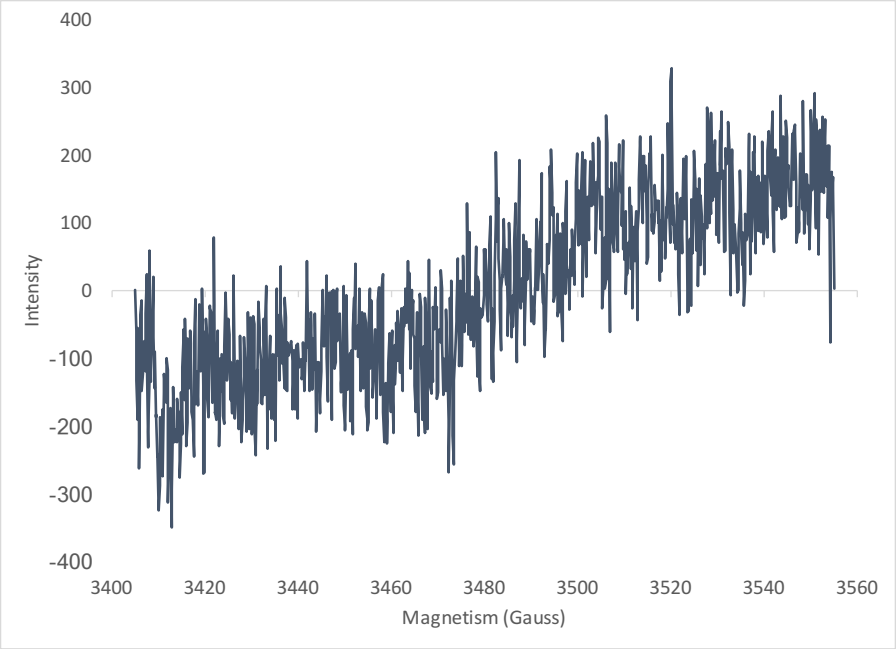

Figure C17: Water blank.

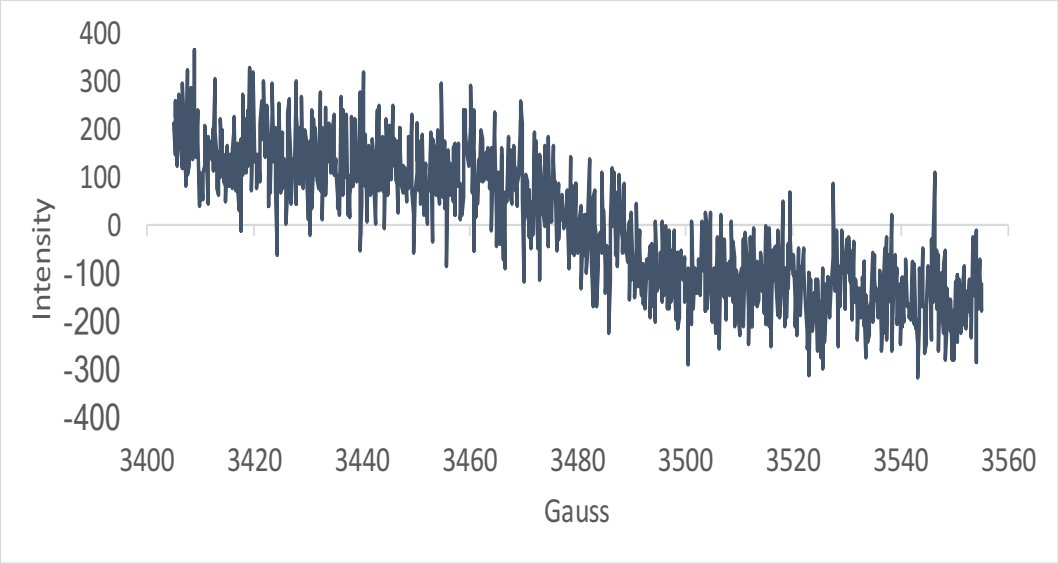

Figure C18: Disodium phosphate.

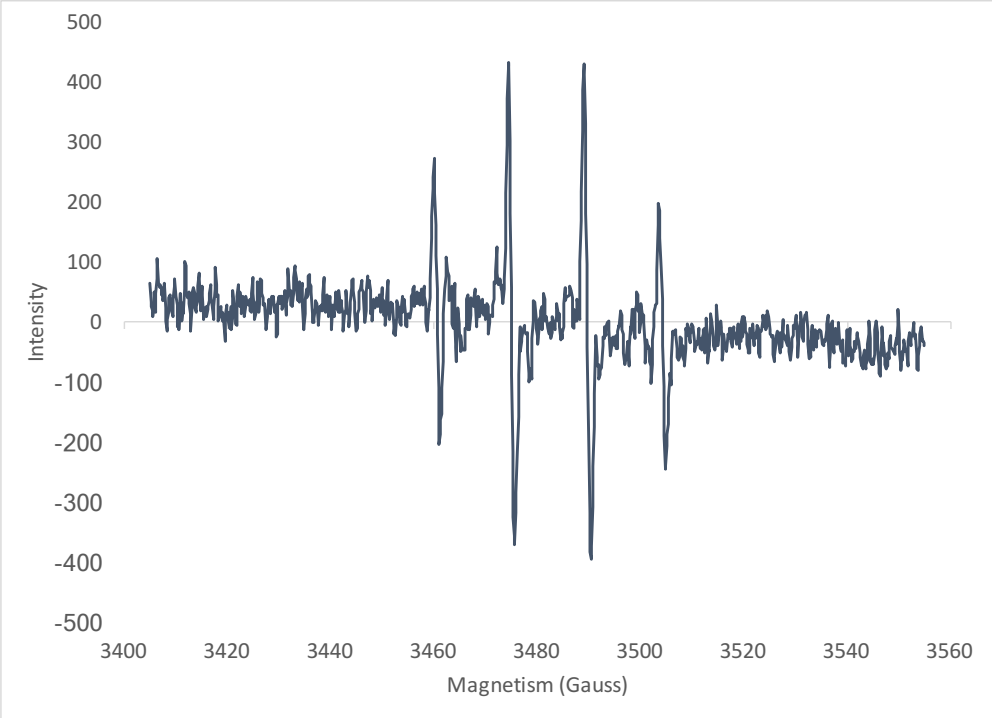

Figure C19: Ozone + hydrogen peroxide activated with UV light.

Bibliography

Abe, A., 1999. Distribution of 1, 4-dioxane in relation to possible sources in the water environment. Sci. Total Environ. 227, 41–47.

Adams, C.D., Scanlan, P.A., Secrist, N.D., 1994. Oxidation and biodegradability enhancement of 1, 4-dioxane using hydrogen peroxide and ozone. Environ. Sci. Technol. 28, 1812–1818.

Adamson, D.T., Piña, E.A., Cartwright, A.E., Rauch, S.R., Hunter Anderson, R., Mohr, T., Connor, J.A., 2017. 1,4-Dioxane drinking water occurrence data from the third unregulated contaminant monitoring rule. Sci. Total Environ. 596–597, 236–245. https://doi.org/10.1016/j.scitotenv.2017.04.085

Anderson, R.H., Anderson, J.K., Bower, P. a., 2012. Co-occurrence of 1,4-dioxane with trichloroethylene in chlorinated solvent groundwater plumes at US air force installations: Fact or fiction. Integr. Environ. Assess. Manag. 8, 731–737. https://doi.org/10.1002/ieam.1306

Ball, R.G., 2010. Soil and water remediation method and apparatus.

Basumallick, L., Ji, J.A., Naber, N., Wang, Y.J., 2009. The fate of free radicals in a cellulose based hydrogel: detection by electron paramagnetic resonance spectroscopy. J. Pharm. Sci. 98, 2464–2471.

Block, P.A., Brown, R.A., Robinson, D., 2004. Novel activation technologies for sodium

persulfate in situ chemical oxidation, in: Proceedings of the Fourth International Conference on the Remediation of Chlorinated and Recalcitrant Compounds. Columbus, OH: Battelle Press, pp. 24–27.

Block, P. a, Brown, R. a, Robinson, D., 2004. Novel Activation Technologies for Sodium Persulfate. Situ Monterey, 2A–05.

Bowman, R.H., 2001. Ozone-peroxide advanced oxidation water treatment system for treatment of chlorinated solvents and 1, 4-dioxane., in: ABSTRACTS OF PAPERS OF THE AMERICAN CHEMICAL SOCIETY. AMER CHEMICAL SOC 1155 16TH ST, NW, WASHINGTON, DC 20036 USA, pp. U463–U463.

Brigham, W.E., 1974. Mixing Equations in Short Laboratory Cores. https://doi.org/10.2118/4256-PA

Brown, R.A., Robinson, D., Block, P.A., 2004. Simultaneous reduction and oxidation: Combining sodium persulfate with zero valent iron, in: Proceedings, Third International Conference on Oxidation and Reduction Technologies for In-Situ Treatment of Soil and Groundwater (ORTs-3), San Diego, CA, USA, October. pp. 24–28.

Burmaster, D.E., 1982. The new pollution: groundwater contamination. Environ. Sci. Policy Sustain. Dev. 24, 6–36.

Buxton, G.V., Greenstock, C.L., Helman, W.P., Ross, A.B., 1988. Critical Review of rate

constants for reactions of hydrated electrons, hydrogen atoms and hydroxyl radicals ($\cdot OH/\cdot O^-$ in Aqueous Solution. J. Phys. Chem. Ref. Data 17. https://doi.org/10.1063/1.555805

Capellos, C., Bielski, B.H.J., 1972. Kinetic Systems: Mathematical Descriptions of Chemical Kinetics in Solution 138A very handy reference that just contains analy.

Crimi, M.L., Taylor, J., 2007. Experimental evaluation of catalyzed hydrogen peroxide and sodium persulfate for destruction of BTEX contaminants. Soil Sediment Contam. 16, 29–45.

Czapski, G., Bielski, B.H.J., 1963. THE FORMATION AND DECAY OF H2O3 AND HO2 IN ELECTRON-IRRADIATED AQUEOUS SOLUTIONS1. J. Phys. Chem. 67, 2180–2184.

DiGuiseppi, W., Whitesides, C., 2007. Treatment options for remediation of 1, 4-dioxane in groundwater. Env. Eng Appl Res Pr. 2, 1–7.

Draper, W.M., Dhoot, J.S., Remoy, J.W., Kusum Perera, S., 2000. Trace-level determination of 1,4-dioxane in water by isotopic dilution GC and GC-MS. Analyst 125, 1403–1408. https://doi.org/10.1039/B002345K

Duwelius, R.F., Yeskis, D.J., Wilson, J.T., Robinson, B.A., 2002. Geohydrology, water quality, and simulation of ground-water flow in the vicinity of a former waste-oil refinery near Westville, Indiana, 1997-2000. US Geological Survey.

Eberle, D., Ball, R., Boving, T.B., 2016. Peroxone activated persulfate treatment of 1, 4-

dioxane in the presence of chlorinated solvent co-contaminants. Chemosphere 144, 728–735.

Eberle, D.E.H., 2015. ISCO of volatile organic contaminants using peroxone activated persulfate and cyclodextrin. University of Rhode Island.

EPA, 1995. Chemical Fact Sheet for 1,4-Dioxane.

EPA, U., 2008. Fact sheet emerging contaminant- 1,4-Dioxane, solid waste and emergency response. Washington, DC.

EPA, U.S., 2013. The third unregulated contaminant monitoring rule (UCMR 3): data summary. EPA, Washingt. DC.

Ferrarese, E., Andreottola, G., Oprea, I.A., 2008. Remediation of PAH-contaminated sediments by chemical oxidation. J. Hazard. Mater. 152, 128–139.

Fetter, C.W., Boving, T., Kreamer, D., 2017. Contaminant hydrogeology. Waveland Press.

Fubini, B., Bolis, V., Giamello, E., Pugliese, L., Volante, M., 1989. The Formation of Oxygen Reactive Radicals at the Surface of the Crushed Quartz Dusts as a Possible Cause of Silica Pathogenicity BT - Effects of Mineral Dusts on Cells, in: Mossman, B.T., Bégin, R.O. (Eds.), . Springer Berlin Heidelberg, Berlin, Heidelberg, pp. 205–214. https://doi.org/10.1007/978-3-642-74203-3_27

Furman, O.S., Teel, A.L., Watts, R.J., 2010. Mechanism of base activation of persulfate. Environ. Sci. Technol. 44, 6423–6428.

Gandesbery, T., Hetzel, F., Smith, R., Riege, L., 1998. Ambient concentrations of toxic chemicals in San Francisco Bay sediments. Calif. Environ. Prot. Agency, Reg. Water Qual. Control Board, San Fr. Bay Reg.

Glaze, W.H., Wallace, J.L., 1984. Control of trihalomethane precursors in drinking water: granular activated carbon with and without preozonation. J. Am. Water Works Assoc. 68–75.

Harbour, J.R., Chow, V., Bolton, J.R., 1974. An electron spin resonance study of the spin adducts of OH and HO2 radicals with nitrones in the ultraviolet photolysis of aqueous hydrogen peroxide solutions. Can. J. Chem. 52, 3549–3553.

He, X., Mezyk, S.P., Michael, I., Fatta-Kassinos, D., Dionysiou, D.D., 2014. Degradation kinetics and mechanism of β-lactam antibiotics by the activation of H 2 O 2 and Na 2 S 2 O 8 under UV-254nm irradiation. J. Hazard. Mater. 279, 375–383.

HSDB, 1995. 1,4-Dioxane [WWW Document]. 1,4-Dioxane. URL http://toxnet.nlm.nih.gov/cgi-bin/sis/search2/r?dbs+hsdb:@term+@DOCNO+81 (accessed 11.18.17).

Huang, K.-C., Couttenye, R.A., Hoag, G.E., 2002. Kinetics of heat-assisted persulfate oxidation of methyl tert-butyl ether (MTBE). Chemosphere 49, 413–420.

Huang, K.-C., Zhao, Z., Hoag, G.E., Dahmani, A., Block, P.A., 2005. Degradation of volatile organic compounds with thermally activated persulfate oxidation. Chemosphere 61,

551–560.

Huling, S.G., Pievetz, B.E., 2006. In-Situ Chemical Oxidation, 1–58. Eng. Issue, EPA United States Environ. Prot. Agency.

IARC, 1999. Re-evaluation of some organic chemicals, hydrazine and hydrogen peroxide. World Health Organization.

ITRC, I., 2005. Technical and Regulatory Guidance for In Situ Chemical Oxidation of Contaminated Soil and Groundwater. Counc. TITaR, Ed.

Jackson, R.E., Dwarakanath, V., 1999. Chlorinated Decreasing Solvents: Physical-Chemical Properties Affecting Aquifer Contamination and Remediation. Groundw. Monit. Remediat. 19, 102–110.

Jaeger, C.D., Bard, A.J., 1979. Spin trapping and electron spin resonance detection of radical intermediates in the photodecomposition of water at titanium dioxide particulate systems. J. Phys. Chem. 83, 3146–3152.

Klečka, G.M., Gonsior, S.J., 1986. Removal of 1, 4-dioxane from wastewater. J. Hazard. Mater. 13, 161–168.

Kolthoff, I.M., Miller, I.K., 1951. The Chemistry of Persulfate. I. The Kinetics and Mechanism of the Decomposition of the Persulfate Ion in Aqueous Medium1. J. Am. Chem. Soc. 73, 3055–3059. https://doi.org/10.1021/ja01151a024

Kraybill, H.F., 1978. Carcinogenesis induced by trace contaminants in potable water. Bull.

N. Y. Acad. Med. 54, 413.

Latimer, W.M., 1938. Oxidation states of the elements and their potentials in aqueous solutions.

Liang, C.J., Bruell, C.J., Marley, M.C., Sperry, K.L., 2003. Thermally activated persulfate oxidation of trichloroethylene (TCE) and 1, 1, 1-trichloroethane (TCA) in aqueous systems and soil slurries. Soil sediment Contam. An Int. J. 12, 207–228.

Liang, S.H., Kao, C.M., Kuo, Y.C., Chen, K.F., Yang, B.M., 2011. In situ oxidation of petroleum-hydrocarbon contaminated groundwater using passive ISCO system. Water Res. 45, 2496–2506.

McGrane, W., 1997. Advanced oxidation processes for destruction and enhanced biodegradability of 1, 4-dioxane. Chem Oxid 6, 231–245.

Mohr, T.K.G., 2001. 1, 4-Dioxane and Other Solvent Stabilizers White Paper. St. Cl. Val. Water Dist. St. Cl. Val. Water Dist.

Mohr, T.K.G., Stickney, J.A., DiGuiseppi, W.H., 2016. Environmental investigation and remediation: 1, 4-dioxane and other solvent stabilizers. CRC Press.

Mottley, C., Mason, R.P., 1988. Sulfate anion free radical formation by the peroxidation of (Bi) sulfite and its reaction with hydroxyl radical scavengers. Arch. Biochem. Biophys. 267, 681–689. https://doi.org/10.1016/0003-9861(88)90077-X

Peyton, G.R., 1993. The free-radical chemistry of persulfate-based total organic carbon

analyzers. Mar. Chem. 41, 91–103.

Rivas, F.J., 2006. Polycyclic aromatic hydrocarbons sorbed on soils: a short review of chemical oxidation based treatments. J. Hazard. Mater. 138, 234–251.

Schroth, M.H., Istok, J.D., Ahearn, S.J., Selker, J.S., 1996. Characterization of Miller-similar silica sands for laboratory hydrologic studies. Soil Sci. Soc. Am. J. 60, 1331–1339.

SERDP, 2011. In Situ Chemical Oxidation for Groundwater Remediation, vol 3. New York, NY.

SERDP, 2006. Remediation, Final Report: Expert Panne Workship on Reducing the Uncertainty of DNAPL Source Zone Remediation. Arlington, VA.

Shen, W., Wang, Y., Zhan, J., Wang, B., Huang, J., Deng, S., Yu, G., 2017. Kinetics and operational parameters for 1, 4-dioxane degradation by the photoelectro-peroxone process. Chem. Eng. J. 310, 249–258.

Siegrist, R.L., 2001. Principles and practices of in situ chemical oxidation using permanganate. Battelle Press.

Simonich, S.M., Sun, P., Casteel, K., Dyer, S., Wernery, D., Garber, K., Carr, G., Federle, T., 2013. Probabilistic analysis of risks to us drinking water intakes from 1, 4-dioxane in domestic wastewater treatment plant effluents. Integr. Environ. Assess. Manag. 9, 554–559.

Stefan, M.I., Bolton, J.R., 1998. Mechanism of the degradation of 1, 4-dioxane in dilute

aqueous solution using the UV/hydrogen peroxide process. Environ. Sci. Technol. 32, 1588–1595.

Stepien, D.K., Diehl, P., Helm, J., Thoms, A., Püttmann, W., 2014. Fate of 1,4-dioxane in the aquatic environment: From sewage to drinking water. Water Res. 48, 406–419. https://doi.org/10.1016/j.watres.2013.09.057

Suh, J.H., Mohseni, M., 2004. A study on the relationship between biodegradability enhancement and oxidation of 1,4-dioxane using ozone and hydrogen peroxide. Water Res. 38, 2596–2604. https://doi.org/10.1016/j.watres.2004.03.002

Suthersan, S., Quinnan, J., Horst, J., Ross, I., Kalve, E., Bell, C., Pancras, T., 2016. Making strides in the management of “emerging contaminants.”

Tsitonaki, A., Petri, B., Crimi, M., Mosbæk, H., Siegrist, R.L., Bjerg, P.L., 2010. In situ chemical oxidation of contaminated soil and groundwater using persulfate: a review. Crit. Rev. Environ. Sci. Technol. 40, 55–91.

US EPA, 2011. Exposure factors handbook 2011 edition (Final). Washington, DC.

Waisner, S., Medina, V.F., Morrow, A.B., Nestler, C.C., 2008. Evaluation of chemical treatments for a mixed contaminant soil. J. Environ. Eng. 134, 743–749.

Wyard, S.J., Smith, R.C., Adrian, F.J., 1968. ESR Spectrum of HO2 in Solutions of Hydrogen Peroxide in Water at 77° K. J. Chem. Phys. 49, 2780–2783.

Zeng, Q., Dong, H., Wang, X., Yu, T., Cui, W., 2017. Degradation of 1, 4-dioxane by

hydroxyl radicals produced from clay minerals. J. Hazard. Mater. 331, 88–98. https://doi.org/10.1016/j.jhazmat.2017.01.040

Zenker, M.J., Borden, R.C., Barlaz, M.A., 2003. Occurrence and treatment of 1, 4-dioxane in aqueous environments. Environ. Eng. Sci. 20, 423–432.

Zhong, H., Brusseau, M.L., Wang, Y., Yan, N., Quig, L., Johnson, G.R., 2015. In-situ Activation of Persulfate by Iron Filings and Degradation of 1,4-dioxane. Water Res. 83, 104–111. https://doi.org/10.1016/j.watres.2015.06.025